Doctoral Dissertation
(Shinshu University)

Study on blood pressure measurement using optical fiber sensor

March 2020

Kyoko KATAYAMA

Interdisciplinary Graduate School of Science and Technology,

Shinshu University

Department of Mathematics and System Development

Contents

Chapter 1

Introduction

1.1. Research background

In 2016, the average life expectancy at birth of Japanese men and women was 81.0 and 87.1 respectively. On the other hand, the health life expectancy at birth of Japanese men and women was 72.1 and 74.8 years respectively. The health life expectancy at birth means the life period without health problems [1-1]. There is approximately 10 years gap between the life expectancy and the health life expectancy. Both the life expectancy and the health life expectancy have become long, but the gap has not changed much since 2001 [1-1]. Living in unhealthy state ruins not only happiness of life but also quality of life. Considering that population aging is expected to accelerate even further in Japan, the medical expenses and grant of nursing care payment are estimated to further increase in the future [1-2], [1-3]. The problem of the gap between the life expectancy and the health life expectancy is not merely the Japanese problem but also the global problem. In 2016, the global average life expectancy at birth was 69.8 years for males and 74.2 years for females. However, the global health life expectancy at birth was 62.0 years for males and 64.8 years for females [1-4]. There is also approximately 10 years gap between two expectancies. The global aging is well-known problem, the population rate over 65 years old is estimated to reach 17.8 % in 2060 [1-5]. Therefore, closing the gap between the average life expectancy and the health life expectancy is a global task to be solved.

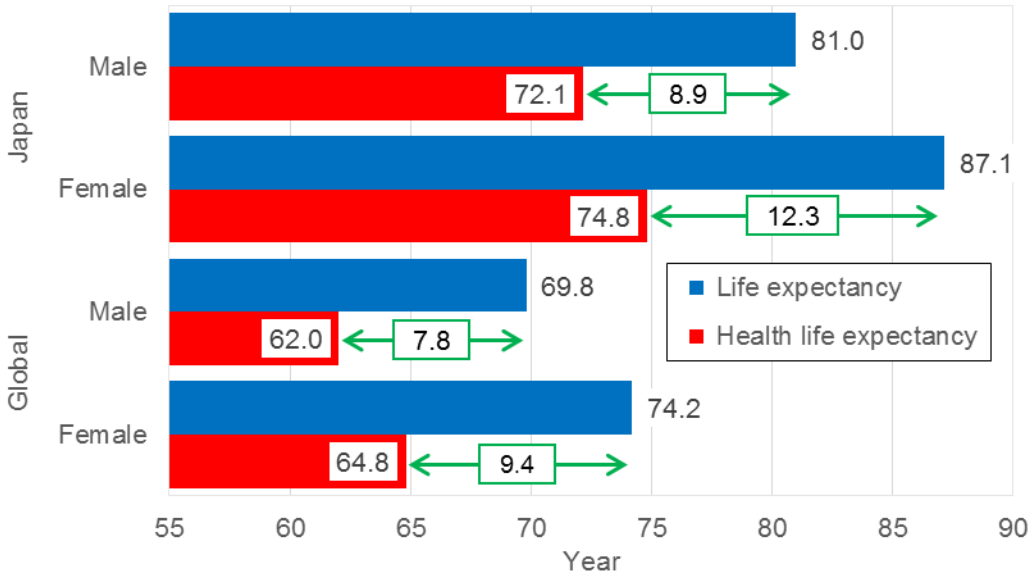

Figure 1-1. Gap between life expectancy and health life expectancy in 2016

The advancement of age and the shortage of doctor have result in increased demand for home healthcare which adapt to lifestyle and preventive medical care for preventing disease through self-care and health maintenance [1-6]–[1-8]. Moreover, the single-person households are globally on the rise. The amount of single-person households is estimated to increase. Especially, the percentage of elderly people living alone is predicted to increase with the aging of society [1-5], [1-9]–[1-11]. Aging certainly leads to lower physical function. Therefore, the elderly person needs more careful healthcare than the young. Especially, in case of single-person householders, it is difficult to deal with emergencies such as sudden illness. To prevent the sudden illness, the daily health check is effective because the daily health check can find small changes in physiology. Thinking that the number of patient with hypertension increases with aging, it is important to grasp the standard of own blood pressure.

According to the survey by Ministry of Health, Labour and Welfare in Japan, the number of the patients suffering from hypertensive diseases is approximately 10 million, and the medical expenses for these patients are above 1.7 trillion yen in 2017 [1-2], [1-12]. The Japanese Society of Hypertension estimated that the number of person with hypertension was approximately 43 million. Therefore, if persons have hypertension, most of them do not visit a medical institution. Same as in Japan, there are many people who have hypertension in the world. According to the survey by World Health Organization, over 1 billion people worldwide are estimated to have hypertension, and 1 in 4 men and 1 in 5 women had hypertension in 2015 [1-13]. Hypertension is called a "silent killer." As its name suggests, hypertension may have no warning signs or symptoms and most people with hypertension could not be aware of the problem. If hypertension state continues, various symptoms such as early morning headaches, nosebleeds, irregular heart rhythms, vision changes, and buzzing in the ears occur. When hypertension advances in severity, it can run fatigue, nausea, vomiting, confusion, anxiety, chest pain, and muscle tremors. Moreover, it increases risk of various complications and leads to deadly diseases. Continuation of hypertension burdens blood vessel. Then, it loses the elasticity and flexibility of blood vessel, increases thickness of blood vessel wall. This is the arteriosclerosis by hypertension. This arteriosclerosis occurs not only at large blood vessel but also at small blood vessel. Moreover, the heart is forced to stand high blood pressure and cardiac hypertrophy occurs [1-14]. Consequently, hypertension causes heart disease and cerebrovascular disease. The top 2 global cause of death was ischemic heart disease and stroke [1-15]. As mentioned above, hypertension

is major risk of these diseases. For these reasons, regular blood pressure measurement is essential to prevent such dreadful diseases. The blood pressure strongly depends on the physical and mental health conditions. Additionally, some hypertension is difficult to find by the blood pressure measurement at the medical checkup or the medical institution. For example, “nocturnal hypertension,” blood pressure does not drop at night and “early-morning hypertension,” blood pressure does not drop even in the early morning. Therefore, continuous monitoring is desirable to notice the early signs of diseases. Furthermore, it is recommended to measure blood pressure at home because blood pressure measured at home has higher ability to predict stroke risk than that measured in the health examination [1-16].

1.2. Demand for development of health monitoring device and current situation

To solve problems written above, the quick development of home healthcare support system is task in medical treatment and welfare field. Therefore, the simple vital sign measurement system for home healthcare has been highly demanded [1-7], [1-8], [1-17]. Additionally, the demand of the own healthcare for healthy person has also increased in recent years [1-18]. To fulfill these demands, it is effective to monitor the vital signs. Here, vital sign means the physiological information which plainly indicates health condition. Blood pressure, pulse rate, respiration rate and body temperature are mainly called vital signs. Glucose level, urinary output and consciousness level are also categorized as vital sign since they are necessary for life support [1-19], [1-20]. Vital sign continues to change by physical condition, changes in the autonomic nervous system or change in mental condition such as stress and strain. Therefore, continuous vital sign monitoring is important for health maintenance and for early detection of disease.

Conventional vital sign measurement system has various problems. A big problem of conventional vital sign measurement device is its size or type. Main type of conventional vital sign measurement systems are too big to carry and is a stationary type; hence, they give the user a sense of restraint and continuous measurement is quite difficult [1-7]. Focusing on the conventional blood pressure measurement device, oscillometric method and korotcoff method are commonly used. These methods give pressure on the wrist or upper-arm by cuff for measuring blood pressure. Omron Corporation solved the device size problem

and released a smart watch which can measure blood pressure using ocillometric method [1-21]. However, it is reported that the correct blood pressure value cannot be measured caused by the pressure given by cuff [1-22], [1-23]. Therefore, the cuff-less measurement is preferable for the blood pressure measurement. For the cuff-less blood pressure measurement, the development of the blood pressure measurement device using optical sensor system has been advanced. Emitting the light from light emitting diode (LED) to the skin surface and detecting the reflected or transmitted light by photo diode (PD), the blood volume change in arteries is measured. Suzuki and Oguri adapted a multiple regression analysis to calculate estimation equation of blood pressure from individual information and features of photoplethysmograph signal in each class [1-24]. Atomi et al. reported the experiments that blood pressure value was estimated from the feature amount of pulse wave measured by plethysmogram and individual information such as age, height, and weight [1-25]. The blood pressure estimation methods by analyzing the feature amount of photoplethysmograph by machine learning were also presented [1-26], [1-27]. However, optical measurement system also has various problems. The system has serious disadvantage that the absolute value of blood volume change cannot be measured [1-28]. It is greatly affected by skin color and moisture such as perspiration, and low-temperature burn caused by the light source energy and the pressure when fixing prove has also been confirmed [1-29]. The cuff-less blood pressure measurement methods using pulse transit time (PTT), pulse wave velocity (PWV) or pulse arrival time (PAT) were also reported [1-30]–[1-32]. These methods are not suitable for the wearable measurement because of two reasons. They need to use optical sensor which may

hurt skin and to fix two or more sensors such as electrocardiogram.

1.3. Advantages of vital sign measurement using FBG sensor

As written above, the vital sign measurement system has various problem to be solved and the many researchers have tackled them. However, each vital sign measurement system are studied separately and the study for multi vital sign measurement system using only one sensor is hardly exist. Increasing the demand and importance for vital sign measurement, the development of measurement system which can monitor as many vital signs as possible at once is desirable. My research group has used fiber Bragg grating (FBG) sensor aiming development of wearable, non-invasive and continuous multi vital sign measurement system. FBG sensor is generally used for strain detection of architecture. I employed it as a vital sign sensor. Just by attaching it on the surface of skin, small change of pulse pressure can be detected. FBG sensor is an optical-fiber-type strain sensor, and small, low-cost, have excellent corrosion resistance and have no risk of low temperature burns. Moreover, it is not affected by water, can detect strain with high sensitivity and high accuracy. These features are suitable for the developing wearable vital sign sensor. Taking advantage of the sensor shape, it can be incorporated into the woven fabric [1-33], [1-34]. Therefore, if the smart cloth which is inserted the FBG sensor is realized, the unconscious and continuous measurement will be possible in daily life. Furthermore, FBG sensor is not affected by electromagnetic noise. Therefore, using optical fiber, increasing the length of the interval between detection part and sensor part, FBG sensor system can used with magnetic resonance imaging (MRI) which gives an electromagnetic effect and in special environments such as high concentration oxygen room where electronic device cannot be used. It means that continuous

vital sign measurement while using various medical inspection devices can be realized by using the FBG sensor. For these reasons, FGB sensor system is applicable for both of general home and medial institution.

1.4. Outline of this study

The goal of this study is a development wearable multi vital sign measurement device and its prevalence. The purpose of this dissertation was to improve the blood pressure measurement function using FBG sensor system and to widen the applicability of FBG sensor system as a multi vital sign measurement device.

Chapter 2, I investigated the relationships between the pulse wave signal obtained by the FBG sensor and the second derivative of the plethysmogram (SDPTG) signal. Comparing the pulse wave signal obtained by the FBG sensor with the SDPTG signal, I confirmed whether the signal measured by the FBG sensor can be used for the vascular age and arteriosclerosis estimation as well as the SDPTG signal.

The verification whether FBG sensor system can trace sudden blood pressure change was performed in Chapter 3. The abrupt blood pressure change was simulated by the cold pressor test. The verification was essential as a wearable and continuous blood pressure monitoring device because the abrupt change in blood pressure burdens the blood vessel and causes of onset of hypertension and dreadful disease such as stroke and heart attack.

Two experiments aiming to improve the accuracy of blood pressure value estimation and to make the FBG sensor system versatile were performed in Chapter 4 and 5. To make our system generally applicable, it is necessary to establish blood pressure estimation method adapted not for individual but for people in general. Therefore, in Chapter 4, estimation result with Partial Least Square Regression (PLSR) and with Artificial Neural Network (ANN) were

compared. Furthermore, I constructed the calibration curve by Partial Least Square Regression (PLSR) with classified pulse wave signal and non-classified pulse wave signal to know whether the classification of pulse wave signal pattern is effective for improving the blood pressure value estimation. I calculated the blood pressure value using the two calibration curves and compared the results in Chapter 5.

In Chapter 6, a summary of this dissertation is presented.

1.5. References

[1-1] “Annual Report on the Ageing Society: 2018 (Summary),” Cabinet Office, Government of Japan. [Online]. Available: https://www8.cao.go.jp/kourei/english/annualreport/2018/2018pdf_e.html. [Accessed: 02-Nov-2019].

[1-2] “Estimates of National Medical Care Expenditure, FY 2017,” Ministry of Health, Labour and Welfare. [Online]. Available: https://www.mhlw.go.jp/toukei/saikin/hw/k-iryohi/17/. [Accessed: 03-Nov-2019].

[1-3] “Status Report of Insured Long-Term Care Service, 2017,” Ministry of Health, Labour and Welfare. [Online]. Available: https://www.mhlw.go.jp/topics/kaigo/osirase/jigyo/17/index.html. [Accessed: 03-Nov-2019].

[1-4] “GHO | By category | Healthy life expectancy (HALE) - Data by WHO region,” WHO. [Online]. Available: http://apps.who.int/gho/data/view.main.HALEXREGv?lang=en. [Accessed: 27-Nov-2019].

[1-5] “2019 White paper on aging society,” Cabinet Office, Government of Japan. [Online]. Available: https://www8.cao.go.jp/kourei/whitepaper/w-2019/html/zenbun/index.html. [Accessed: 03-Nov-2019].

[1-6] “The World Health Report 2006 - working together for health,” World Healthcare Organization, 2006. [Online]. Available: https://www.who.int/whr/2006/whr06_en.pdf?ua=1. [Accessed: 02-Nov-2019].

[1-7] Y. Ken-Ichi, “Progress of Non-invasive, Ambulatory, and Non-conscious Biomedical Measurement,” J. Jpn. Soc. Precis. Eng., vol. 62, no. 11, pp. 1525–1529, Nov. 1996, doi: 10.2493/jjspe.62.1525.

[1-8] Yahagi N., Vital care network - Life saving network, vol. 9. Nature interface, 2002.

[1-9] “People in the EU – who are we and how do we live?,” eurostat. [Online]. Available: https://ec.europa.eu/eurostat/statistics-explained/index.php?title=People_in_the_EU_%E2%80%93_who_are_we_and_how_do_we_live%3F. [Accessed: 03-Nov-2019].

[1-10] “LATEST DEMOGRAPHIC STATICS 2019,” National Institute of Population and Social Security Research. [Online]. Available: http://www.ipss.go.jp/syoushika/tohkei/Popular/Popular2019.asp?chap=0. [Accessed: 03-Nov-2019].

[1-11] “The Future Consumer Households in 2030,” EUROMONITOR INTERNATIONAL. [Online]. Available: https://go.euromonitor.com/rs/805-KOK-719/images/sbFutureConsumerHouseholds2030.pdf?mkt_tok=eyJpIjoiTldabFkyWXdOalZtWm1RdyIsInQiOiJkN0ZDMHUxYkszMzlTblhVT29EbExRcWkzYm1jRVhxb1VBbjBxOUtnWFwvbEpCKzhjeTdNTlFFZlhXdVBVZWgzMUZ2RWNYUFd1QXBhQlRzQlU4TnluQlwvNGxcL1pcL2M4eWlGNGh2cTZXSFRTMmZsZTZiUlRRWUdDOGNNM1wvN0RVUDNkIn0%3D.

[1-12] “2017 Summary of Patient Survey,” Ministry of Health, Labour and Welfare. [Online]. Available: https://www.mhlw.go.jp/toukei/list/10-20.html. [Accessed: 03-Nov-2019].

[1-13] “World Health Statistics 2015,” WHO. [Online]. Available: http://www.who.int/gho/publications/world_health_statistics/2015/en/. [Accessed: 03-Nov-2019].

[1-14] “Hypertension,” National Cerebral and Cardiovascular Center Hospital. [Online]. Available: http://www.ncvc.go.jp/hospital/pub/knowledge/disease/hypertension.html. [Accessed: 28-Nov-2019].

[1-15] “Mortality and global health estimates,” WHO. [Online]. Available: http://www.who.int/gho/mortality_burden_disease/en/. [Accessed: 03-Nov-2019].

[1-16] T. Ohkubo et al., “How many times should blood pressure be measured at home for better prediction of stroke risk? Ten-year follow-up results from the Ohasama study,” J. Hypertens., vol. 22, no. 6, pp. 1099–1104, Jun. 2004, doi: 10.1097/00004872-200406000-00009.

[1-17] Hosaka H., “Health information system using wearable sensors,” Micromechatronics, vol. 47, no. 1, pp. 47–51, 2003, doi: 10.20805/micromechatronics.47.1_47.

[1-18] “Guide for the smooth execution of special medical checkup and specific health guidance (third edition),” Ministry of Health, Labour and Welfare. [Online]. Available: https://www.mhlw.go.jp/stf/seisakunitsuite/bunya/0000172888.html. [Accessed: 03-Nov-2019].

[1-19] Tokuda Y., Dr. Tokuda’s vital sign course. Japan Medical Journal, 2013.

[1-20] Kuwahara M., Redo vital signs. Medicus shuppan, 2016.

[1-21] “HeartGuide | Wearable Blood Pressure Monitor,” Omron. [Online]. Available: https://omronhealthcare.com/products/heartguide-wearable-blood-pressure-monitor-bp8000m/. [Accessed: 21-Nov-2019].

[1-22] Y. Inagaki, “Current status and issues of biological monitoring equipment,” Jpn. J. Med. Instrum., vol. 86, no. 6, pp. 517–525, 2016, doi: 10.4286/jjmi.86.517.

[1-23] O. Shirasaki, “Role and evluation of sphygmomanometer in circulatory organ field,” Jpn. J. Med. Instrum., vol. 80, no. 6, pp. 622–631, 2010, doi: 10.4286/jjmi.80.622.

[1-24] S. SUZUKI and K. OGURI, “Cuffless Blood Pressure Estimation based on Photoplethysmograph Signal by Classifying on account of Cardiovascular Characteristics,” IEICE Tech. Rep., vol. 108, no. 371, pp. 1–4, Dec. 2008.

[1-25] K. Atomi, H. Kawanaka, Md. S. Bhuiyan, and K. Oguri, “Cuffless Blood Pressure Estimation Based on Data-Oriented Continuous Health Monitoring System,” Comput. Math. Methods Med., vol. 2017, pp. 1–10, Apr. 2017, doi: 10.1155/2017/1803485.

[1-26] J. C. Ruiz-Rodríguez et al., “Innovative continuous non-invasive cuffless blood pressure monitoring based on photoplethysmography technology,” Intensive Care Med., vol. 39, no. 9, pp. 1618–1625, Sep. 2013, doi: 10.1007/s00134-013-2964-2.

[1-27] Q. Xie, G. Wang, Z. Peng, and Y. Lian, “Machine Learning Methods for Real-Time Blood Pressure Measurement Based on Photoplethysmography,” in 2018 IEEE 23rd International Conference on Digital Signal Processing (DSP), 2018, pp. 1–5, doi: 10.1109/ICDSP.2018.8631690.

[1-28] H. IWATA and M. HIRAI, “Photoplethysmography,” Japanese College of Angiology, vol. 45, no. 5, pp. 329–332, May 2005.

[1-29] T. Ukawa, “Current State and Problems of Pulse Oximetry,” Jpn. J. Med. Instrum., vol. 77, no. 2, pp. 52–59, Feb. 2007.

[1-30] H. Gesche, D. Grosskurth, G. Küchler, and A. Patzak, “Continuous blood pressure measurement by using the pulse transit time: comparison to a cuff-based method,” Eur. J. Appl. Physiol., vol. 112, no. 1, pp. 309–315, Jan. 2012, doi: 10.1007/s00421-011-1983-3.

[1-31] F. Cattivelli and H. Garudadri, “Noninvasive Cuffless Estimation of Blood Pressure from Pulse Arrival Time and Heart Rate with Adaptive Calibration,” presented at the Proceedings - 2009 6th International Workshop on Wearable and Implantable Body Sensor Networks, BSN 2009, 2009, pp. 114–119, doi: 10.1109/BSN.2009.35.

[1-32] H. Lin, W. Xu, N. Guan, D. Ji, Y. Wei, and W. yi, “Noninvasive and Continuous Blood Pressure Monitoring Using Wearable Body Sensor Networks,” IEEE Intell. Syst., vol. 30, pp. 1–1, Nov. 2015, doi: 10.1109/MIS.2015.72.

[1-33] S. Koyama, A. Sakaguchi, H. Ishizawa, Y. Kurumi, H. Oshiro, and H. Kimura, “Vital Sign Measurement Using Covered FBG Sensor Embedded into Knitted Fabric for Smart Textile,” J. Fiber Sci. Technol., vol. 73, no. 11, pp. 300–308, 2017, doi: 10.2115/fiberst.2017-0046.

[1-34] A. Sakaguchi, M. Kato, H. Ishizawa, H. Kimura, and S. Koyama, “Fabrication of Optical Fiber Embedded Knitted Fabrics for Smart Textiles,” J. Text. Eng., vol. 62, no. 6, pp. 129–134, 2016, doi: 10.4188/jte.62.129.

Chapter 2

Classification of Pulse Wave Signal Measured by FBG Sensor for Vascular Age and Arteriosclerosis Estimation

2.1. Introduction

In recent years, the increase in medical expenses has become a social problem owing to the increase in the aging population [2-1]. The medical expenses of patients with circulatory system diseases is over 5.9 trillion yen, and the estimated number of patients per day in medical care institutions is over 1 million in Japan [2-2], [2-3].

In particular, arteriosclerosis causes circulatory system diseases—namely, heart diseases such as cardiac infarction and cerebrovascular diseases such as cerebral apoplexy. Blood vessels typically have sufficient elasticity and flexibility to carry oxygen and nutrition. However, due to aging and lifestyle diseases, the elasticity and flexibility is lost and it is the main cause of arteriosclerosis. Moreover, a daily check is essential because arteriosclerosis often has no symptoms. Therefore, a continuous measurement device is desired. Additionally, the measurement device needs to be transportable, noninvasive, and physically unconstraining. Conventional measuring devices have limitations such as stationarity and the physical stress generated by the cuff.

One simple method for estimating the degree of arteriosclerosis exists, which uses the second derivative of the plethysmogram (SDPTG) signal. The plethysmogram expresses a change in the volume of blood. However, the plethysmogram has the problem that its reading is difficult because the base line sway is large, and the inflection point of the waveform has little undulation. In contrast, the base line oscillation of SDPTG is small and the inflection point of the waveform is emphasized [2-4], [2-5]. The shape of the SDPTG signal is known to change according to the blood circulation state, age, or past medical history.

Using the relative value of the inflection point of the SDPTG signal, the vascular age is estimated. This method can be applied with a conventional acceleration pulse wave meter. However, the photoelectric plethysmogram wave meter is affected by the skin color and sweat. Furthermore, it only measures the amount of oxyhemoglobin and does not record any other vital sign information.

To overcome these limitations of conventional devices, I proposed a wearable device that can measure multiple vital signs using a fiber Bragg grating (FBG) sensor. The FBG sensor is an optical-fiber-type strain sensor, which has a high sensitivity and precision. Noninvasive and physically unconstrained measurement is possible because the FBG sensor is extremely thin and light. Moreover, the sensor is not affected by electromagnetic noise. Therefore, it can be used in special environments such as magnetic resonance imaging (MRI) rooms, making it is suitable for continuous vital sign measurement.

Various medical applications that involve the use of the FBG sensor have been extensively developed. Witt et al. reported a medical textile with an FBG sensor for monitoring the respiratory movement [2-6]; Ho et al. presented an FBG-based vascular access device that specializes in arterial localization [2-7]. Presti et al. proposed an FBG-based wearable system for both respiratory and cardiac monitoring [2-8]. Lukasz et al. monitored the vital signs of patients during an MRI survey by using an FBG sensor [2-9]. Elsarnagwy et al. presented embedded FBG sensors that are used to simultaneously measure vital signals such as respiration, heartbeat, and body motion signals in the form of a smart costume [2-10].

In previous studies, the usefulness of FBG sensors for various vital sign

measurements was demonstrated [2-11]–[2-18]. It was found that an FBG sensor could measure the signal corresponding to the expansion and contraction of an artery—namely, the pulse wave—just by attaching it to the surface of the skin. By performing a multivariate analysis to the pulse wave signals, the blood pressure and blood glucose level can be calculated. The shape of the pulse wave signal obtained by the FBG sensor resembles that of the SDPTG signal [2-11]. The purpose of study in this chapter is to confirm whether the signal measured by the FBG sensor can be used to estimate the vascular age and arteriosclerosis, similar to the signal measured by the SDPTG signal, by comparing the tendency of the pulse wave signal with that measured by the SDPTG signal. I focused on the shapes of the pulse wave signals measured by the FBG sensor and then classified them into seven patterns according to the classification of Sano et al. [2-4]. In this chapter, I present the results of the influences of age progression and the blood pressure in the shape of the signal. Further, I compare the tendency of the shape change with that of the SDPTG signal. The addition of the system for estimating the vascular age and arteriosclerosis to my multiple-vital-sign measurement system using the FBG sensor aids in the realization of improved health monitoring.

2.2. Principles of the FBG Sensor System

In this experiment, I used FBG sensor systems (PF25-S01, PF20: Nagano Keiki, Inc., Tokyo, Japan) and an amplified spontaneous emission (ASE) light source. Figure 2-1 shows a schematic of the sensor part. The FBG is the periodic change in the refractive index constructed in the core of the optical fiber and works as a wavelength-selective mirror. Broadband near-infrared light is emitted from the ASE light source and propagates through the optical fiber. The only wavelength that is reflected in the FBG is called the Bragg wavelength λ_B, which is expressed as

$$\lambda_B = 2n_{eff.}\Lambda \quad (1)$$

where $n_{eff.}$ is the effective refractive index of the grating in the fiber core and Λ is the grating interval. When pressure is applied to the sensor, the grating interval changes. Therefore, the Bragg wavelength also changes according to (1). The effective refractive index is 1.5, the measurement range is 1550 ± 0.5 nm, and the length of the sensor part is 10 mm.

Figure 2-2 shows the optical system of the PF25-S01 FBG sensor system. A shift in the Bragg wavelength is detected as an interference phase shift by the Mach–Zehnder interferometer. Then, the change in the strain of the sensor part is calculated using the wavelength shift [2-19], [2-20]. The resolutions of the wavelength shift and distortion are 0.1 pm and 0.08 μstrain, respectively [2-21]. Figure 2-3 shows a schematic of the PF-20 FBG sensor system. The Bragg wavelength is measured by comparing the light reflected from the FBG sensor with the light output from the wavelength reference unit. Then, the change in the strain of the sensor part is calculated using the wavelength shift. The resolutions

of the wavelength shift and distortion are 0.1 pm and 0.08 μstrain, respectively [2-21]. These high strain measurement systems enable the measurement of pulse waves. In this experiment, the amplitude of the FBG signal related to the strain induced by a pulse is more than 2 pm. Therefore, considering that the resolution of the wavelength shift is 0.1 pm, the signal-to-noise ratio is 26 dB [2-11].

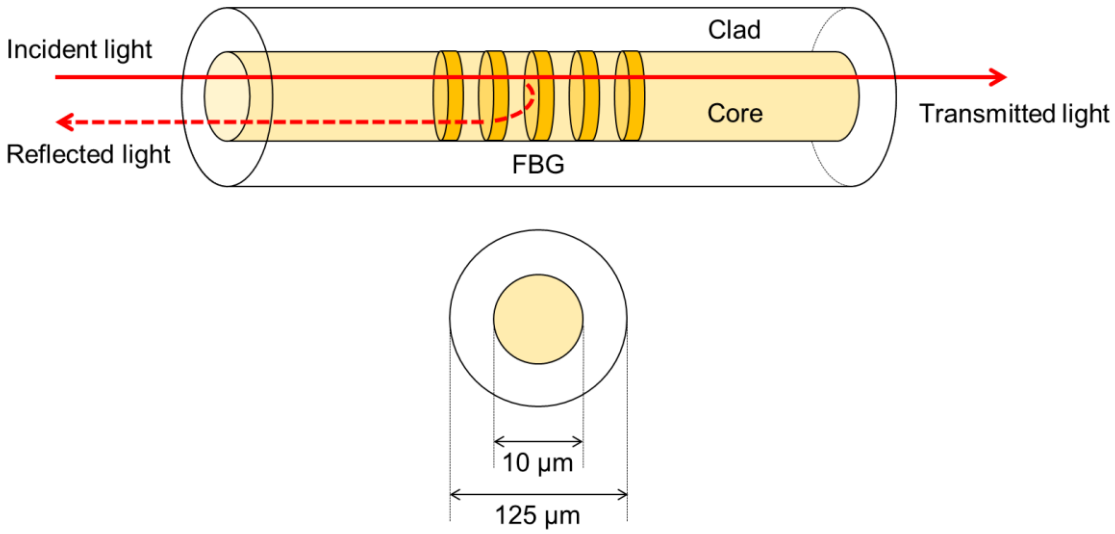

Figure 2-1. Schematic of the sensor part

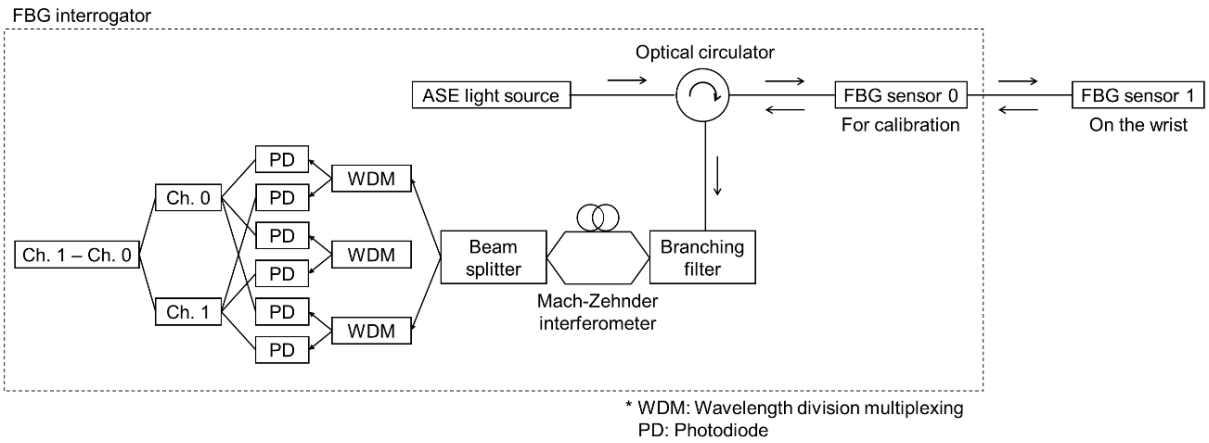

Figure 2-2. Optical system of the PF25-S01 FBG sensor system

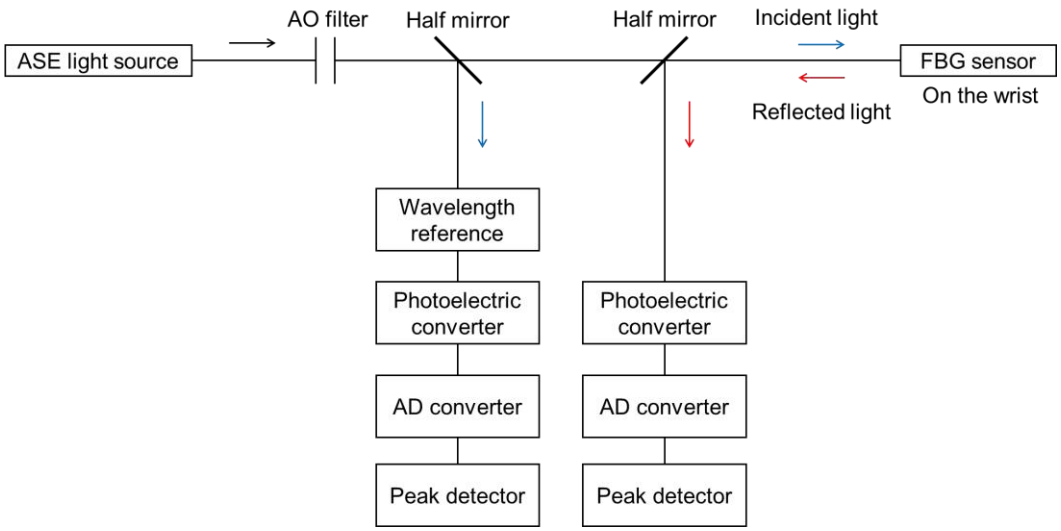

Figure 2-3. Schematic of the PF20 FBG sensor system

2.3. Experimental Methods

The FBG sensor needs to be fixed at a pulsation point to measure a pulse wave signal. The surface of the human body has several pulsation points such as those at the wrist and neck [2-22]. The pressure in the blood vessels due to the blood flow propagates at these pulsation points well. In previous studies, we confirmed that pulse waves could be measured at these points using the FBG sensor [2-11]–[2-18]. In this chapter, I fixed the FBG sensor on the surface of the wrist using medical adhesive tape, as depicted in Figure 2-4, and measured the pulse wave signals. The pulsation points near the heart were not chosen in this chapter because the movement of the lungs due to respiration is detected as noise by the FBG sensor.

A total of 195 persons (113 males and 82 females) aged 21–89 years were recruited in this chapter, and they were chosen at random for the experiment. The measurement position was the sitting or supine position according to the subject's condition. The subjects stayed completely still and barely made any body movement during the measurements. The reference blood pressure was measured at the upper arm using a blood pressure pulse wave inspection apparatus (VS-1500N: FUKUDA DENSHI, Tokyo, Japan) or bedside monitor (PVM-2701: NIHON KOHDEN CORPORATION, Tokyo, Japan) at the same time as the FBG sensor measurements. The relative error in the blood pressure for this reference method was 3%. The measurement time using the FBG sensor was approximately 30 s, which is in accordance with the measurement time of the apparatus used to measure the reference value. The sampling frequencies of the PF25-S01 and PF20 FBG sensor systems were 10 and 1 kHz, respectively.

The pulse wave signal contained background noise such as the noise of the power supply of the interrogator circuit system and small oscillations. To reduce the effect of this noise, a bandpass filter with a frequency of 0.5–5.0 Hz was applied to the pulse wave signal [2-11]–[2-18]. Next, the first derivative of the filtered signal was acquired, which was then divided into one cycle from one peak to the next peak. A divided signal corresponds to a single heartbeat. The divided signals were averaged and normalized over the measurement time. In the normalization, the minimum and maximum points were set to 0 and 1, respectively. In addition, the number of sampling points was adjusted to the fewest number of samples. These signal processes were necessary to remove fluctuations in the pulse wave interval due to the pulse rate and breathing activity and the fluctuations due to the pressure exerted by the FBG sensor on the human body when it is attached. Then, the normalized signals were classified into seven patterns through visual observation according to the classification by Sano et al. [2-4].

The protocol of this study was approved by the Shinshu University Ethics Committee (Project identification code: No. 3202, Verification clinical trial with wearable vital sign measurement system).

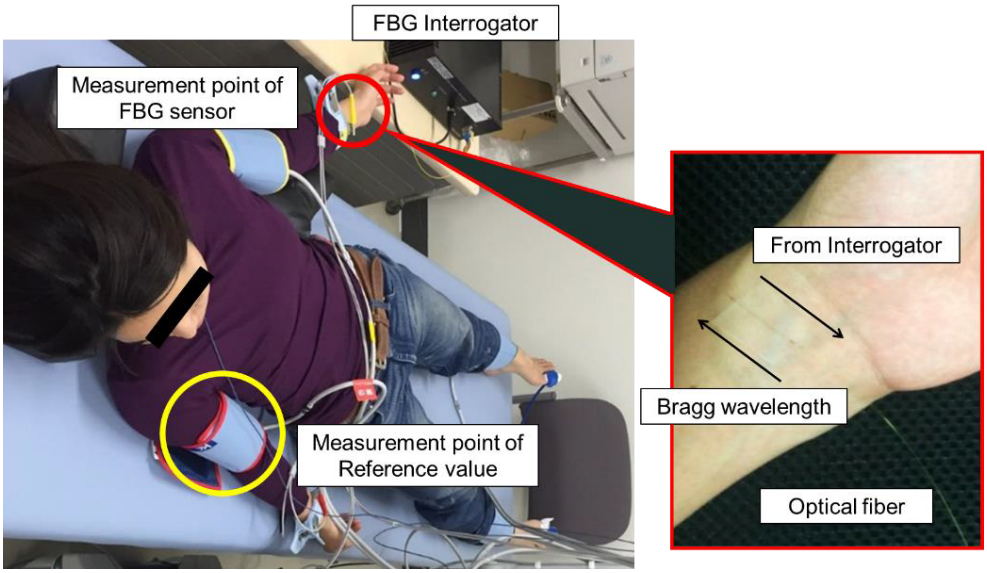

Figure 2-4. Image of measurement using the FBG sensor during the experiment

Table 2-1. The age composition of the subject

		Sex		
		Male	Female	Total
Age	20–29	11	3	14
	30–39	5	7	12
	40–49	3	13	16
	50–59	18	11	29
	60–69	19	15	34
	70–79	31	16	47
	80–89	26	17	43
	Total	113	82	195

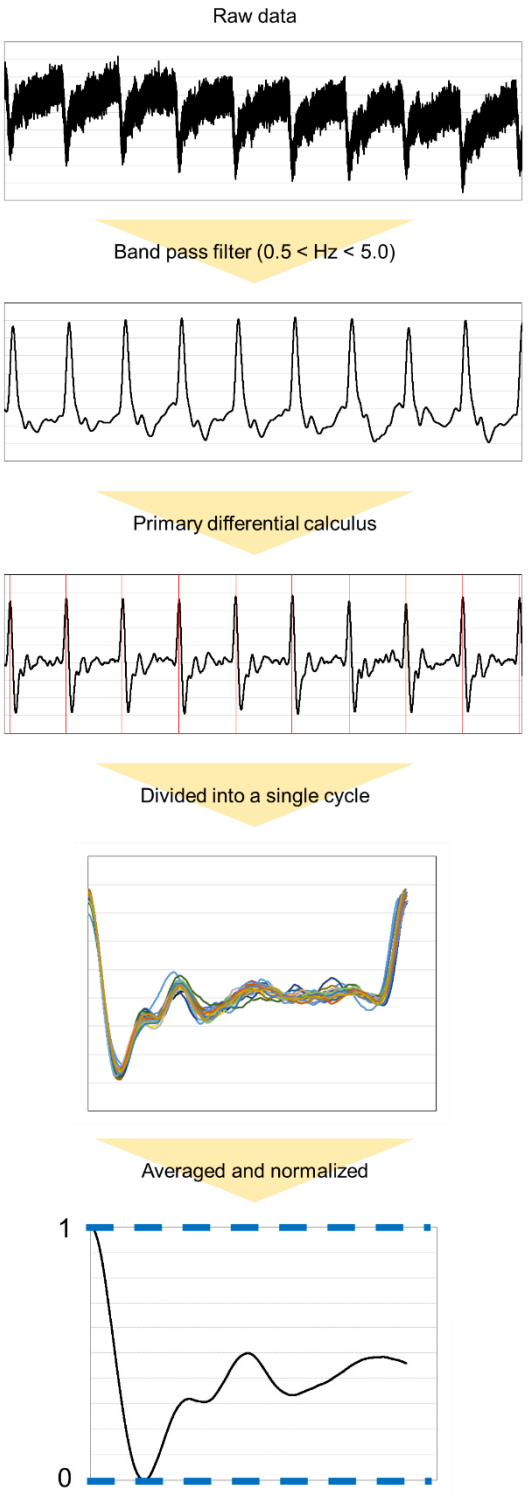

Figure 2-5. Signal processing flow

2.4. Experimental Results and Discussion

2.4.1.Pulse Wave Signal Classification

Figure 2-6 depicts the peaks (indicated as a toe) of the SDPTG signal. Peaks a and b are the systolic anterior components, which correspond to the drive pressure wave due to heart contraction. Peaks c and d are the systolic posterior components, which correspond to the drive pressure wave reflected from the peripheral vessel. Peak e is a diastolic anterior component [2-23]. Sano et al. reported that the acceleration pulse wave can be classified into seven patterns: A–G, as depicted in Figure 2-7. They reported that as circulation becomes worse or as aging progresses, the shape of the acceleration pulse wave changes from pattern A to pattern G [2-4]. A patient with high blood pressure tends to exhibit patterns C–G, which implies that the patient has poor blood circulation. Further, a patient with a vascular disease such as cerebrovascular disease and ischemic heart disease tends to exhibit patterns E–F. The conventional photoelectric plethysmogram wave meter uses the relative values of the peaks to estimate the vascular age and the degree of arteriosclerosis. Because the wave shape changes owing to factors such as exercise and medicine dosing, it can be used to evaluate the effects of exercise and medicine dosing.

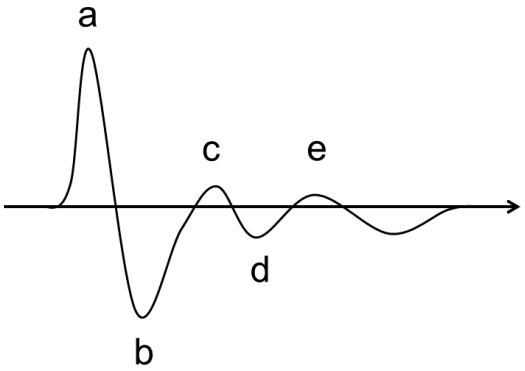

Figure 2-6. Peaks a–e of the SDPTG signal

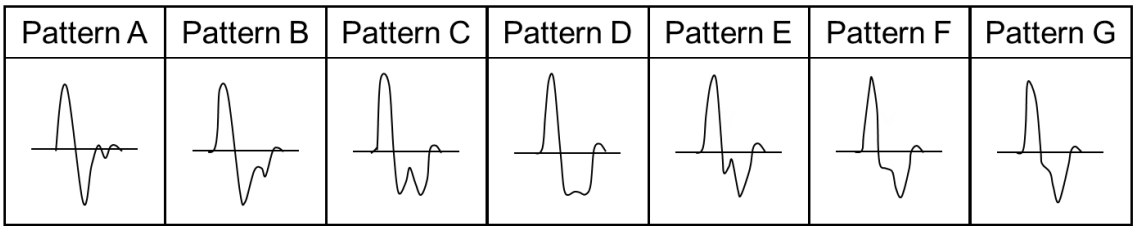

Figure 2-7. Patterns of the SDPTG signal.

Several pulse wave signals obtained by the FBG sensor in this experiment are shown in Figure 2-8. The pulse wave signals have five peaks and are similar to the SDPTG signal. By comparing the signals obtained by the FBG sensor with the classification scheme (Figure 2-7) and following the classification criteria described below, the obtained signals were classified as the most similar pattern. The classification criteria were set as below. First, if the peak b is clearly bigger than peak d, the signal can be classified as pattern A or B. Then, if peak c $\geqq$ 0.5, the signal is classified as pattern A, otherwise as pattern B. Next, if the peak b $\fallingdotseq$ peak d, the signal is classified as pattern C or D and if the peak c $\fallingdotseq$ 0, the signal is classified as pattern C. Finally, if peak b > peak d, the signal can be classified

into pattern E, F or G. Then, if peak b < peak c, the pattern is E; if peak b ≒ peak c, the pattern is F and if peak b > peak c, the pattern is G. This classification is performed by three person and the pattern was determined by majority vote. For instance, the pulse wave signal of Subject 26 was classified as pattern A. Likewise, the pulse wave signals of Subjects 66 and 89 were classified as patterns D and F, respectively. Eventually, the pulse wave signals of all 195 subjects were classified, as presented in Table 2-2.

Table 2-2. Classification Results of Pulse Wave Signals Obtained by the FBG Sensor Pattern

		Pattern							
		A	B	C	D	E	F	G	Total
Age	20–29	10	4	0	0	0	0	0	14
	30–39	2	8	0	1	0	1	0	12
	40–49	3	8	0	2	0	3	0	16
	50–59	7	9	2	10	0	1	0	29
	60–69	4	6	2	6	2	8	6	34
	70–79	4	13	3	19	2	4	2	47
	80–89	9	7	2	12	2	7	4	43
	Total	39	55	9	50	6	24	12	195

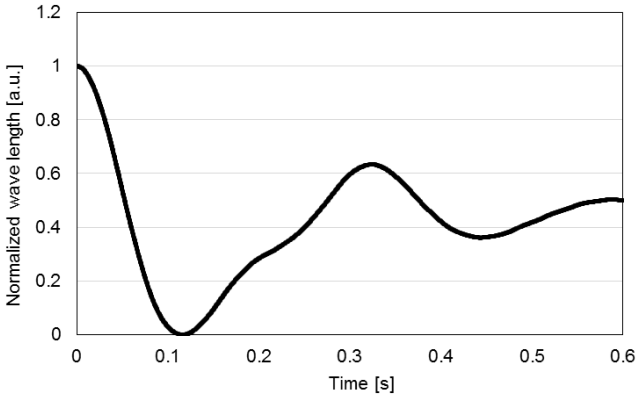

(a)

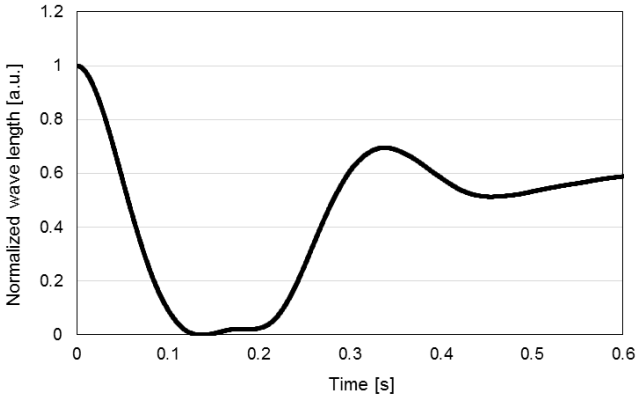

(b)

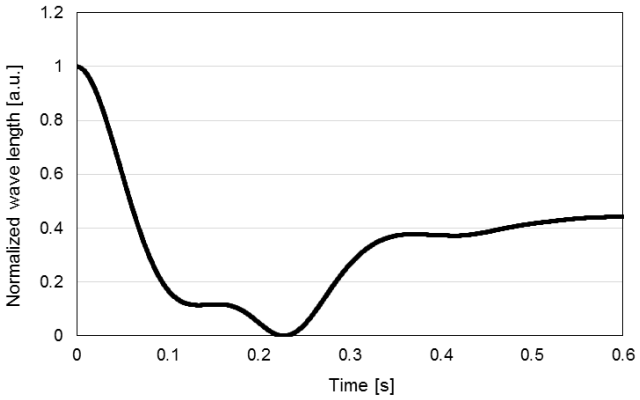

(c)

Figure 2-8. Normalized pulse wave signals for Subjects (a) 26, (b) 66, and (c) 89

2.4.2. Change in the Shape of the Pulse Wave Signal Measured by the FBG Sensor According to Age

The pulse wave signal measured by the FBG sensor was classified into seven patterns, A–G, as presented in Table 2-2. Figure 2-9 shows the percentages of wave shape patterns for various age groups. Subjects in their 20s and 30s tended to exhibit patterns A or B, and the percentages for the other patterns were low. However, as age increased, the percentages for patterns A and B decreased, and those for patterns C–G increased. This tendency corresponds to that of the SDPTG signal [2-4]. Therefore, the change in blood circulation with the increase in age can be reflected in the change in the shape of the pulse wave signal measured by the FBG sensor and enable the blood circulatory dynamics to be evaluated from changes in the waveform.

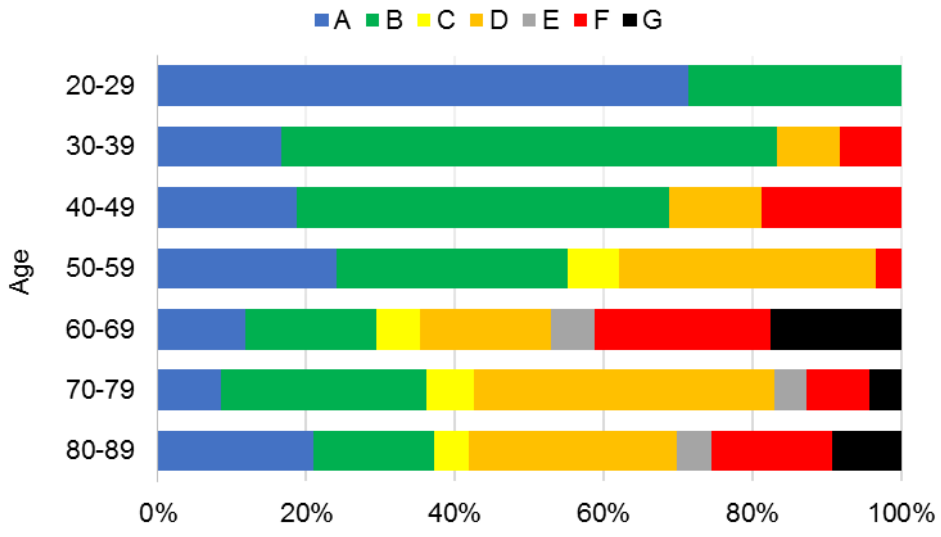

Figure 2-9. Percentages of the wave shape patterns according to age group for the signals measured by the FBG sensor

2.4.3. Change in the Shape of the Pulse Wave Signal Measured by the FBG Sensor According to the Blood Pressure Level

According to the blood pressure levels set forth by the World Health Organization, I classified the pulse wave signals measured by the FBG sensor as normal, high-normal, and hypertensive blood pressure (Table 2-3). The classification results are shown in Figure 2-10.

All patterns were observed at all blood pressure levels. However, as the blood pressure level worsened, the percentages of patterns E–G increased. This result was also similar to that for the SDPTG signal [2-4]. This implies that while the pattern of the pulse wave signal measured by the FBG sensor does not change with only the change in the blood pressure, subjects with a high blood pressure tend to exhibit a pattern that suggests poor blood circulation.

Although the plethysmogram detects the amount of change in oxyhemoglobin, the FBG sensor measures the strain on the surface of the skin due to the change in the volume of an artery. Moreover, the strain is induced on the surface of the skin by the pressure exerted by the blood flow in the blood vessel. In other words, the pulse wave signal measured by the FBG sensor has information related to the blood flow and the flexibility of the blood vessel, which is why the blood pressure and blood glucose level can be predicted by the FBG sensor. Therefore, the pulse wave signal measured by the FBG sensor has more information than the plethysmogram.

Table 2-3. Classification of blood pressure level by WHO

	SBP	DBP	Condition
Normal	~ 129	~ 84	Satisfy both condition
High-Normal	130 ~ 139	85 ~ 89	Satisfy at least one of condition
Hypertensive	140 ~	90 ~	Satisfy at least one of condition

* SBP: Systolic blood pressure, DBP: Diastolic blood pressure

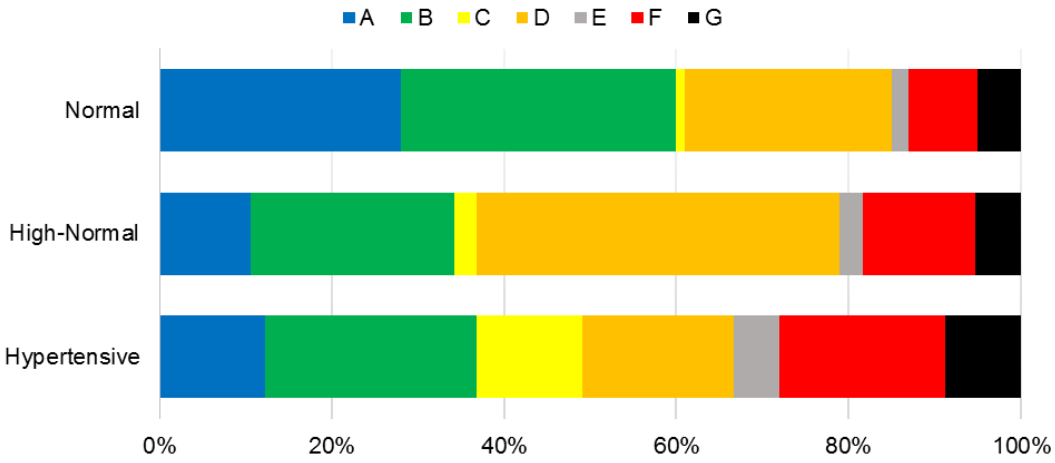

Figure 2-10. Percentages of the wave shape patterns according to blood pressure level for signals measured by the FBG sensor

2.5. Conclusion

In this chapter, I focused on the shape of the pulse wave signal measured by an FBG sensor to confirm whether it can be used to estimate the vascular age and arteriosclerosis. The pulse wave signals measured by the FBG sensor were classified into seven patterns according to the classification of Sano et al. [2-4]. Then, I confirmed the effects of age and blood pressure on the change in the shape of the signal. As age increases and the blood pressure level becomes high, the shape of the pulse wave signal measured by the FBG sensor tends to exhibit a pattern indicating poor blood circulation. This tendency is the same as that of the SDPTG signal. Considering that the SDPTG signal is used to estimate the vascular age and arteriosclerosis, the pulse wave signal measured by the FBG sensor can also be used to estimate these quantities. To verify this, I need to practically compare the vascular age and the degree of arteriosclerosis predicted using the pulse wave signal measured by an FBG sensor with the reference data measured by a conventional device. Moreover, it is necessary to obtain data over wide ranges of vascular ages and degrees of arteriosclerosis to test our system thoroughly. Therefore, experiments need to be performed with healthy subjects and subjects with circulatory system diseases. Furthermore, I need to clarify how the shape of the pulse wave changes with the blood pressure. However, it is difficult to measure subjects with optional blood pressures. Therefore, it is necessary to examine measurements with an artificial blood vessel for which the optional blood pressure can be modified. Additionally, by measuring an artificial blood vessel, which simulates arteriosclerosis, I can clarify the mechanism of the change in the shape of the pulse wave due to arteriosclerosis.

The conventional photoelectric pulse wave sensor is capable of continuous measurement; however, it is affected by skin color and sweat. As mentioned above, this sensor only measures the amount of oxyhemoglobin and does not record any other vital sign information. In contrast, as the FBG sensor measures strain information influenced by the blood flow and the flexibility of blood vessels, it can predict other vital signs such as the blood pressure and blood glucose levels [2-11]–[2-18]. In this chapter, it is found that the FBG multiple-vital-sign measurement system can also evaluate the condition of the blood vessel. Furthermore, the shape of the sensor is suitable for use as a wearable device. I have already developed a method for incorporating this sensor into clothes such as a wristband. Nevertheless, the FBG-based system still has drawbacks related to the interrogation unit, which is bulky and limits the portability and transportability of the system. To overcome this drawback, it was suggested a wireless portable FBG interrogation system employing an optical edge filter [2-24]. Therefore, this sensor system can simultaneously monitor multiple vital signs, implying that the FBG sensor can monitor health more comprehensively. It has to be mentioned that the signal measured by the FBG sensor also has the information related to the fixing pressure by medical adhesive tape. However, the optimal fixing pressure of the FBG sensor and how much the pressure effect on the pulse wave signal are not clear yet. Therefore, the experiment which changes the fixing pressure gradually has to be carried out to find the optimal fixing pressure for the continuous measurement. When the optimal fixing pressure is found, the stable acquisition of the pulse wave signal becomes easy and the accuracy of vital sign estimation can improve.

2.6. References

[2-1] "Annual Report on the Aging Society: 2015 (Summary)," Cabinet Office, Government of Japan. [Online]. Available: https://www8.cao.go.jp/kourei/english/annualreport/2015/2015pdf_e.html.

[2-2] "2014 Summary of Patient Survey," Ministry of Health, Labour and Welfare. [Online]. Available: https://www.mhlw.go.jp/english/database/db-hss/sps_2014.html. [Accessed: 01-Nov-2019].

[2-3] "Estimates of National Medical Care Expenditure, FY 2015," Ministry of Health, Labour and Welfare. [Online]. Available: https://www.mhlw.go.jp/toukei/saikin/hw/k-iryohi/15/index.html. [Accessed: 01-Nov-2019].

[2-4] S. Yuji et al., "Evaluation of peripheral circulation with accelerated plethysmography and its practical application. | Article Information | J-GLOBAL," J Sci. Labor, vol. 61, no. 3, pp. 129–143, 1985.

[2-5] H. Sachiko, I. Shoji, K. Takayoshi, and I. Haruo, "Relationship Between Accelerated Plethysmogram, Blood Pressure and Arteriolar Elasticity," J Sci. Labor, vol. 41, no. 1, pp. 98–107, 1992, doi: 10.7600/jspfsm1949.41.98.

[2-6] J. Witt et al., "Medical Textiles With Embedded Fiber Optic Sensors for Monitoring of Respiratory Movement," IEEE Sens. J., vol. 12, no. 1, pp. 246–254, Jan. 2012, doi: 10.1109/JSEN.2011.2158416.

[2-7] S. C. M. Ho, W. Li, M. Razavi, and G. Song, "Fiber Bragg grating based arterial localization device," Smart Mater. Struct., vol. 26, no. 6, p. 065020, May 2017, doi: 10.1088/1361-665X/aa6ec2.

[2-8] D. L. Presti et al., "Wearable System Based on Flexible FBG for Respiratory and Cardiac Monitoring," IEEE Sens. J., vol. 19, no. 17, pp. 7391–7398, Sep. 2019, doi: 10.1109/JSEN.2019.2916320.

[2-9] Ł. Dziuda, M. Krej, and F. W. Skibniewski, "Fiber Bragg Grating Strain Sensor Incorporated to Monitor Patient Vital Signs During MRI," IEEE Sens. J., vol. 13, no. 12, pp. 4986–4991, Dec. 2013, doi: 10.1109/JSEN.2013.2279160.

[2-10] T. Elsarnagawy, J. Haueisen, M. Farrag, S. G. Ansari, and H. Fouad, "Embedded Fiber Bragg Grating Based Strain Sensor as Smart Costume for Vital Signal Sensing," Sens. Lett., vol. 12, Nov. 2014, doi: 10.1166/sl.2014.3382.

[2-11] Y. Miyauchi, "Study on development of vital sign measurement system applying optical measurement," Ph.D dissertation, Interdisciplinary Graduate School of Science and Technology, Shinshu University, Nagano,

Japan, 2014.

[2-12] M. Kawamura, H. Ishizawa, S. Sato, and S. Koyama, “Application to vital signs by Fiber Bragg Grating sensing,” presented at the SICE Annual Conference 2011, Tokyo, Japan, 2011, pp. 2702–2704.

[2-13] Y. Miyauchi, H. Ishizawa, S. Sato, and A. Hattori, “Development of the pulse rate measuring system by FBG sensors,” presented at the 10th JSMBE Symposium Nagano district, Nagano, Japan, 2012, pp. 13–14.

[2-14] Y. Katsuragawa and H. Ishizawa, “Non-invasive blood pressure measurement by pulse wave analysis using FBG sensor,” presented at the 2015 IEEE International Instrument and Measurement Technology Conference (I2MTC), Pisa, Italy, 2015, pp. 511–515, doi: 10.1109/I2MTC.2015.7151320.

[2-15] S. Chino, H. Ishizawa, S. Hosoya, S. Koyama, and K. Fujimoto, “Non-invasive blood pressure measurement—The study of measuring points,” presented at the SICE Annual Conference 2016, Tsukuba, Japan, 2016, pp. 1706–1709, doi: 10.3390/s17010048.

[2-16] S. Koyama, H. Ishizawa, K. Fujimoto, S. Chino, and Y. Kobayashi, “Influence of Individual Differences on the Calculation Method for FBG-Type Blood Pressure Sensors,” Sensors, vol. 17, no. 1, Dec. 2016, doi: 10.3390/s17010048.

[2-17] Y. Miyauchi, S. Koyama, and H. Ishizawa, “Basic experiment of blood-pressure measurement which uses FBG sensors,” presented at the 2013 IEEE International Instrumentation and Measurement Technology Conference (I2MTC), Minneapolis, MN, USA, 2013, pp. 1767–1770, doi: 10.1109/i2mtc.2015.7151320.

[2-18] S. Kurasawa, S. Koyama, H. Ishizawa, K. Fujimoto, and S. Chino, “Verification of Non-Invasive Blood Glucose Measurement Method Based on Pulse Wave Signal Detected by FBG Sensor System,” Sensors, vol. 17, no. 12, p. 2702, Dec. 2017, doi: 10.3390/s17122702.

[2-19] Y. Sano and T. Yoshino, “Fast optical wavelength interrogator employing arrayed waveguide grating for distributed fiber Bragg grating sensors,” J. Light. Technol., vol. 21, no. 1, pp. 132–139, Jan. 2003, doi: 10.1109/JLT.2003.808620.

[2-20] Y. Sano and T. Yoshino, “Effect of light source spectral modulation on wavelength interrogation in fiber Bragg grating sensors and its reduction,” IEEE Sens. J., vol. 3, no. 1, pp. 44–49, Feb. 2003, doi: 10.1109/JSEN.2003.809027.

[2-21] M. Todd, G. A. Johnson, and C.-C. Chang, “Passive, light intensity-independent interferometric method for fibre Bragg grating interrogation,” Electron. Lett., vol. 35, pp. 1970–1971, Nov. 1999, doi: 10.1049/el:19991328.
[2-22] S. Hinohara and S. Okada, How to see and read the vital signs. Shorinsha, 2004.
[2-23] E. Mohamed, I. Norton, B. Matt, D. Abbott, and D. Schuurmans, “Detection of a and b waves in the acceleration photoplethysmogram,” Biomed. Eng. OnLine, vol. 13, pp. 139–158, 2014.
[2-24] K. Ogawa, S. Koyama, Y. Haseda, K. Fujita, H. Ishizawa, and K. Fujimoto, “Wireless, Portable Fiber Bragg Grating Interrogation System Employing Optical Edge Filter,” Sensors, vol. 19, no. 14, Jul. 2019, doi: 10.3390/s19143222.

Chapter 3

Verification of Blood Pressure Monitoring System Using Optical Fiber Sensor – Tracing Sudden Blood Pressure Changes –

3.1. Introduction

In Japan, the estimated population of the people who were 65 years old and above was 35,378 thousand by October 1, 2018, and it made up 28.1 % of the total population. This ratio is anticipated to rise to 40 % in 2040 [3-1], [3-2]. This increase in the elderly population will result in higher medical expenses [3-3] and increased demand for the home and preventive medical care. Therefore, it is essential to build a home-care support system that is equipped with vital medical devices for home health monitoring systems.

According to the recent estimates, in Japan, the number of the patients suffering from high blood pressure alone is over 10 million, and the medical expenses for these patients are above 1.8 trillion yen [3-4], [3-5]. The high blood pressure increases the risk for cardiovascular disease and heart diseases caused by arteriosclerosis; hence, it is crucial to monitor the blood pressure to prevent such diseases. The human blood pressure strongly depends on the physical and mental health conditions. Therefore, continuous monitoring is desirable to notice the early signs of diseases. The conventional blood pressure measurement devices have limited mobility, and an application of physical pressure through cuffs is required for their operation. Hence, a portable, non-invasive, and accessible equipment is highly desired for the continuous measurement of blood pressure.

To this end, the development of smart textiles which has a body signal detection function has been widely investigated [3-6]–[3-8]. Markus et al. presented a textile-based pulse oximeter which is consisted of plastic optical fibers into standard fabrics. Witt et al. reported the medical textile into which a

fiber Bragg grating (FBG) sensor for monitoring respiratory movement. We have designed a measurement device using a fiber Bragg grating (FBG) sensor that can measure multiple vital signs [3-9]–[3-14]. We have also suggested the FBG sensor embedded into the knitted fabric and found the potential to use the sensor in smart textile for monitoring vital signs [3-15], [3-16]. The FBG sensor is an optical-fiber-type strain sensor which has high sensitivity and precision. We found that the expansion and contraction of an artery, namely the pulse wave, could be measured by just placing the FBG sensor on the surface of the skin. Noninvasive and straightforward measurement is possible with this device as the FBG sensor is very thin and lightweight. Moreover, the sensor is not affected by the electromagnetic noise; therefore, the sensor can be used in particular environments such as a magnetic resonance imaging room. Hence, the FBG sensor is suitable for continuous blood pressure measurement.

In the previous studies, we have demonstrated the usefulness of the FBG sensor for various vital sign measurements such as heart rates and respiration rates [3-9]–[3-11]. Here, we report the FBG-sensor based blood pressure value prediction method that utilizes the calibration curve obtained by the partial least squares regression (PLSR) of the pulse wave signals measured using the FBG sensor. Then, the blood pressure value can be calculated by substituting the pulse wave signals measured by the FBG sensor into the calibration curve [3-12]–[3-14]. Previously, we have estimated the blood pressure values for the gradual intra-day fluctuations; however, the blood pressure can change suddenly due to illness, exercise, and environmental changes such as a change in temperature. The abrupt change in blood pressure burdens the blood vessel and causes the onset

of hypertension. Therefore, it is essential to validate that our system can trace sudden blood pressure change as a wearable and continuous blood pressure monitoring device.

In this chapter, I demonstrate the detection of a sudden change in blood pressure by the FBG sensor system. I simulated the abrupt change in the blood pressure using the cold pressor test to mimic the actual effects of environmental and physical changes on human blood pressure, and these changes were detected by the shape of the pulse wave signal measured by the FBG sensor to obtain the blood pressure readings. The results indicate that the FBG sensor system was able to detect variations in the blood pressure values through the changes in the shape of the pulse wave signals and, thus, the blood pressure can be predicted with sufficient prediction accuracy.

3.2. Measurement Principle

3.2.1.Principle of the FBG Sensor System

In this chapter, I used an FBG sensor system (PF25-S01: Nagano Keiki, Inc., Tokyo, Japan) and an amplified spontaneous emission (ASE) light source with the wavelength range of 1528–1570 nm. The optical arrangement of the FBG sensor system is shown in Figure 3-1, and the schematic view of the sensor is shown in Figure 3-2. A diffraction grating with alternating high- and low-refractive-index parts at a constant period is created in a section of the optical fiber core as shown in Figure 3-2. The ASE light source emits broadband near-infrared light, which propagate through the optical fiber. The light reaches the FBG sensor through the optical circulator. In the sensor, only a specific wavelength—the Bragg wavelength that satisfies the condition in Eq. (1)—is reflected.

$$\lambda_B = 2n_{eff.}\Lambda \tag{1}$$

where λ_B is the Bragg wavelength; $n_{eff.}$ is the refractive index of the gating part; and Λ is the spacing of the diffraction grating. The spacing of the diffraction grating spacing changes, when the pressure is applied to the sensor. Therefore, the Bragg wavelength (λ_B) also changes according to Equation (1). The shift in the Bragg wavelength is detected as an interference phase shift by the Mach–Zehnder interferometer. The optical path difference is approximately 5 mm. Then, the light is split by a beam-splitter into three components, whose phases differ from each other by (2/3) π. These split light beams are detected via wavelength division multiplexing (WDM). Then, the detected lights are converted into an electric signal using a photodiode (PD), which is subsequently

converted into a digital signal using an A/D converter. The phase angles are demodulated at Ch. 0 and Ch. 1, and the wavelength shift is calculated [3-17], [3-18]. Since, the FBG sensor 0 is inside the detector body, and it is not affected from the external light, the change in the light intensity added to the FBG sensor 1 can be effectively detected by subtracting the intensity obtained by the FBG sensor 0 from that of the FBG sensor 1. The signal from the FBG sensor 0 is used for the temperature correction of the measurement environment. In this system, the resolution of the wavelength shift is 0.1 pm, and the resolution of the distortion is 0.08-μ strain [3-19]. This high strain measurement system enables the measurement of the pulse wave. The system used in this chapter is the same system as it was used in chapter 2.

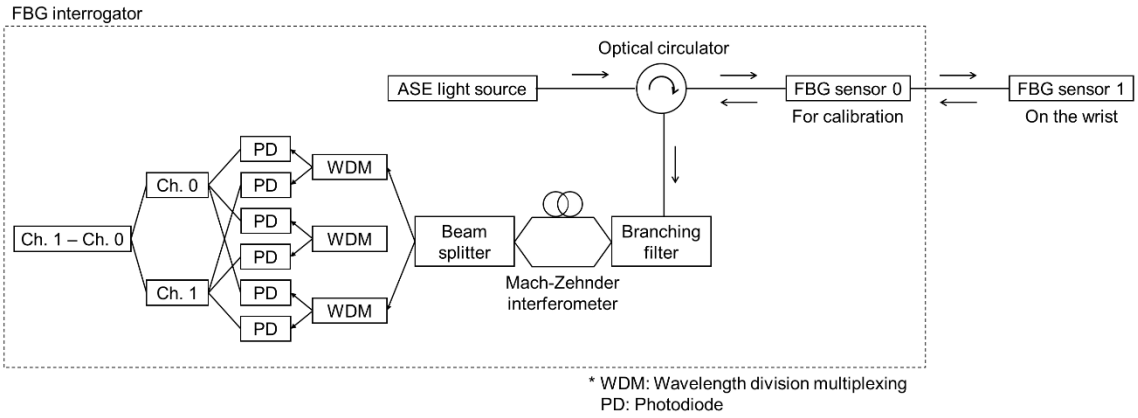

Figure 3-1. Optical arrangement of the FBG sensor system

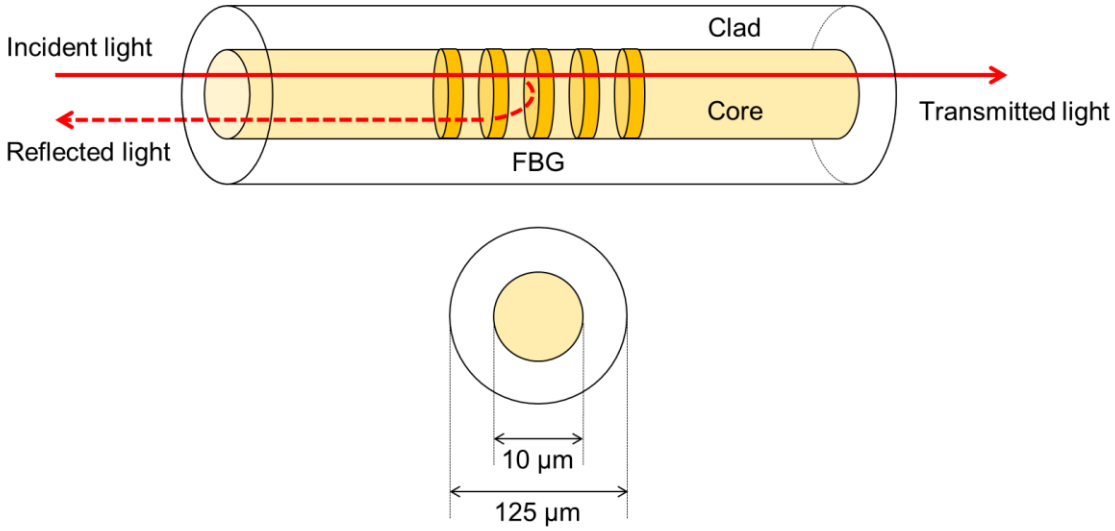

Figure 3-2. Schematic view of the Fiber Bragg Grating (FBG) sensor

3.2.2.Partial Least Squares Regression (PLSR) Method

In this chapter, for the estimation of blood pressure values using the pulse wave data obtained in the previous section, a calibration curve is constructed by the PLSR method from a multivariable analysis software, Pirouette Version 2.0 (InfoMerix, Inc., Woodinville, WA, USA). PLSR is an analytical method which predicts the objective variables from the relation between the objective variables and the explanatory variables [3-20]. The principal component factor is calculated using the explanatory variable and the objective variable, which are assumed to have an error. In this chapter, the pulse wave signals measured by the FBG sensors are used as the explanatory variables, and the reference blood pressure values measured by the bedside monitor is used as the objective variables. The reference blood pressure values have measurement errors; therefore, the PLSR method was used to construct a calibration curve. Firstly, the principal component factor called PLS factor was calculated with the explanatory variables

and the objective variable, and the regression equation was found. Then, the new objective variables were calculated with this regression equation. A new PLS factor was calculated with these new objective variables and explanatory variables. Adding this new PLS factor, the regression equation and objective variables were recalculated. Repeating this calculation, which the number of PLS factor increases, a regression equation whose error is smaller was obtained. The optimal number of PLS factor was determined by the prediction residual sum of squares (PRESS). The cross validation is performed using leave-one-out method. PRESS of the PLS model before and after adding PLS factor was calculated and then verified by the F-test. If there is a significant difference, PLS factor is added, otherwise, the regression equation of the model with a smaller number of factors was selected as the optimal model.

3.3. Experimental Methods

The experimental demonstration of the blood pressure measurement system equipped with the FBG sensors is shown in Figure 3-3. The FBG sensor is a strain sensor. If the sensor is installed at no-distortion point, no signal is measured. Therefore, the sensor must be fixed at the pulsation point to obtain the pulse wave signal. On the surface of a human body, there are several pulsation points such as wrist and neck [3-21]. The pressure in the blood vessels due to blood flow propagates well to these pulsation points. In the previous studies, we have confirmed that the pulse wave could be measured at these points using an FBG sensor [3-9]–[3-11]. I fixed the FBG sensor on the surface of the left wrist over the radial artery using a medical adhesive tape (Figure 3-3) as discussed in our previous studies [3-10]–[3-12], [3-22], and the pulse wave signals were measured. The FBG sensor was installed perpendicular to the flow direction of the radial artery.

The subjects were three healthy men in their twenties (labeled as subjects A, B, C). The measurement position was the sitting position as illustrated in Figure 3-3. The subjects stayed completely still and barely made any body movement during the measurements. At the right upper arm, the reference blood pressure value was measured using the bedside monitor (PVM-2701: NIHON KOHDEN CORPORATION, Tokyo, Japan) simultaneously, while measurements were taken using the FBG sensor. The relative error of the blood pressure value with respect to the reference method is 3%. I performed ten measurements per person. Each measurement with the FBG sensor took approximately 30 s, in accordance with the measurement time of the bedside monitor. The sampling frequency was

10 kHz.

To cause a sudden change in the blood pressure, I used the cold pressor test. The cold pressor test is the method proposed by Hines, E.A. Jr. and Brown, G.E. that tests the functioning of the autonomic nervous system [3-23]. In this experiment, the subjects bathed their feet in cold water from the second to fifth measurement, and they pulled their feet out during the remaining five measurements to allow a sudden change in the blood pressure.

The pulse wave signal obtained using the system had a background noise such as the power supply noise of the interrogator circuit system and other small oscillations. To improve the signal-to-noise ratio, a bandpass filter applied to the pulse wave signal that allowed the band frequencies of 0.5–5.0 Hz to pass through [3-10]–[3-14]. Next, the primary differential calculus was applied to the filtered signal, and the resulting derivative signal was divided into a single cycle from one peak to the next. A divided signal (a single cycle) corresponds to a single heartbeat. The divided signals were averaged and normalized. In the normalization process, the maximum point was set to 1 and the minimum point was set to 0. Additionally, in the horizontal axis, the number of sampling points is unified in the fewest number of samples. To cancel the fluctuations in the time measurements of the single pulse wave signals caused by the pulse rate, respiration, and the attachment pressure of the FBG sensor on the human body, it is important to process these signals as discussed above. Finally, using the processed signal as the explanatory variables and the reference blood pressure values as the objective variables, the calibration curve was constructed with the PLSR method.

The protocol of this study was approved by the Shinshu University Ethics Committee (Project identification code: No. 3202, Verification clinical trial with wearable vital sign measurement system).

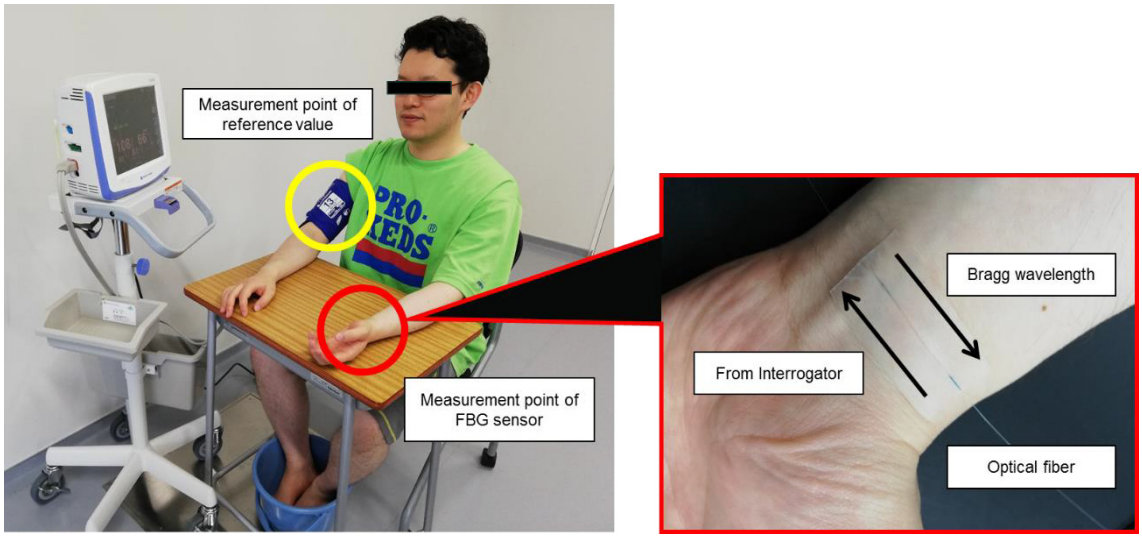

Figure 3-3. Experimental demonstration of blood pressure measurement using the FBG sensor

Table 3-1. Subject's status for each measurement

Measurement	Subject's status
1	Before bathing feet in cold water
2~5	Bathing feet in cold water
6~10	After pulling out feet from out water

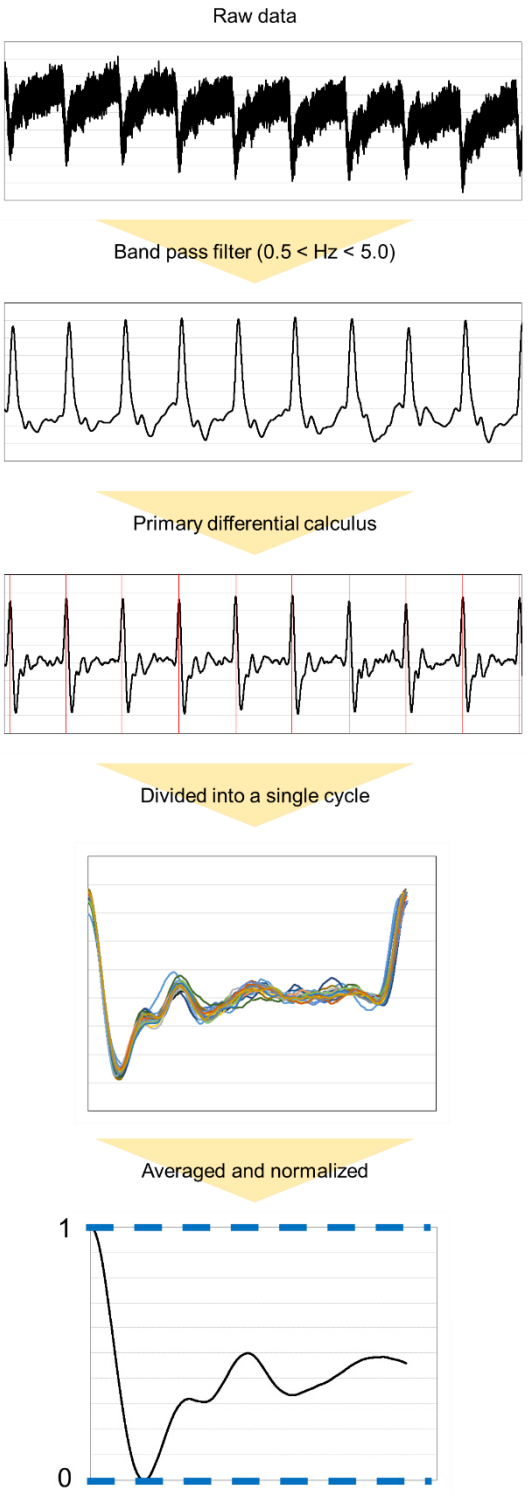

Figure 3-4. Signal processing flow

3.4. Experimental Results and Discussion

3.4.1. Change of Reference Blood Pressure Value by Cold Pressor Test

In Figure 3-4, the change in the reference blood pressure values by the cold pressor test are displayed for all the subjects, namely A, B, and C. The range in gray color is the time when they bathed their feet in cold water.

The systolic blood pressure (SBP) values obtained for all the subjects using the bedside monitor are shown in Figure 3-5 (a). The measurements show that the SBP values increased at first when the subjects bathed their feet in cold water for the second measurement relative to the first measurement taken at rest. During second to fifth measurement, the values were relatively higher (compared with the first measurement at rest), when the subjects kept their feet in the cold water. A gradual decrease in the blood pressure was observed for subjects A and B, when they pulled their feet out of the cold water in subsequent measurements (fifth to sixth measurement), whereas the decrease was rapid for the subject C during this measurement.

The results for the diastolic blood pressure (DBP) values obtained using the bedside monitor are shown in Figure 3-5 (b). The DBP values increased while subjects had their feet in cold water; however the increase was not as large as observed with the SBP values. Additionally, I observed a larger change in the DBP value per measurement from the second measurement to the fifth one (with cold water) compared with the change per measurement from the sixth measurement to the tenth one as evidenced in Figure 3-5 (b).

From there results, I conclude that the individual differences (subject-

dependent) observed in the tendency of the blood pressure change, while subjecting them to the same thermal stimulation, may be associated with the sympathetic nerve activity of each individual.

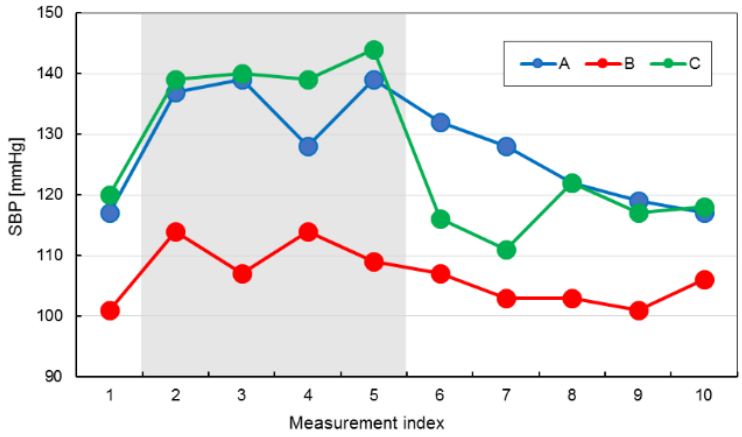

(a)

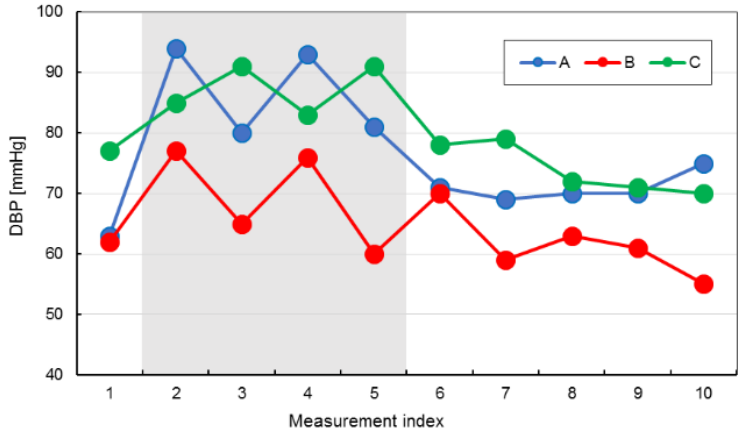

(b)

Figure 3-5. Change in the reference blood pressures: (a) systolic blood pressure (SBP) values; (b) diastolic blood pressure (DBP) values, obtained by the cold pressor test for each subject (A, B, and C)

3.4.2. Shape Change of Pulse Wave Signal Measured by FBG Sensor during a Sudden Blood Pressure Change

Figure 3-6 depicts the pulse wave signals without differential processing (left panels; Figures 3-6 (a), (c), and (e)) and with differential processing (right panels; Figures 3-6 (b), (d), and (f)) for each subject. The differential processing was performed aiming to emphasize the change of waveform. The blue lines indicate the pulse wave signals when the reference blood pressure was low and the red lines indicate the pulse wave signals when the reference blood pressure was high. As evidenced from Figure 3-6, the shape change of the pulse waves are significantly clearer after the differential processing compared with the unprocessed signals. In particular, the change in the pulse wave shape from 0.1 s to 0.3 s can be associated with the change in the blood pressure values. The pulse wave shape during this time range represents the reflected wave from the peripheral blood vessel. When the blood pressure value becomes higher due to the constricted blood vessel, the reflected wave measured by our system becomes larger. Therefore, the reflected wave amplitude represents the influence of blood pressure on the pulse wave. Compared with the pulse wave signals measured by the FBG sensor, the amplitude of the reflected wave (0.1–0.3 s) appeared to be larger, when the reference blood pressure value was higher. Hence, the amplitude of the reflected wave accompanies the increase and decrease in the reference blood pressure values. Therefore, the prediction of the blood pressure values after processing the pulse wave signals measured by the FBG sensor system is a valid approach.

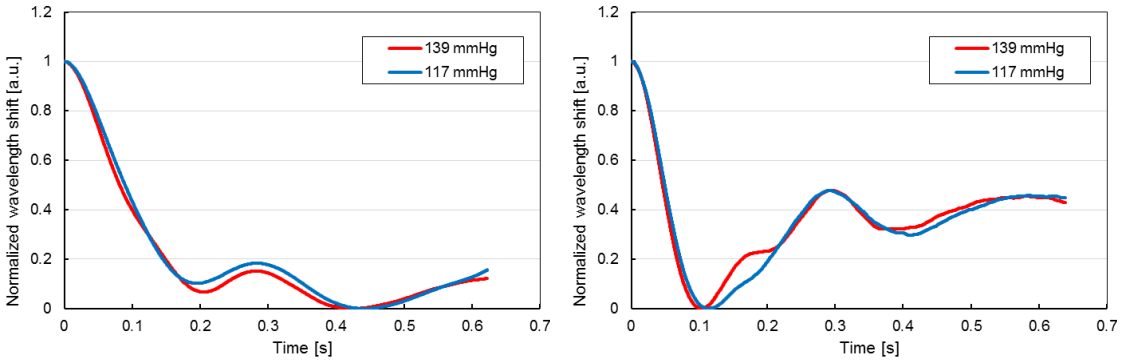

(a)

(b)

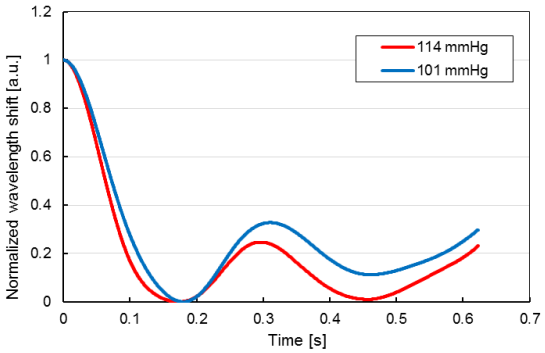

(c)

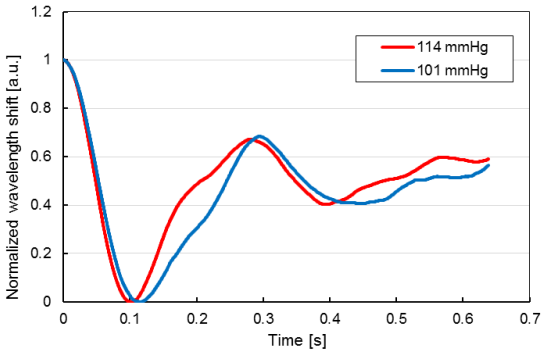

(d)

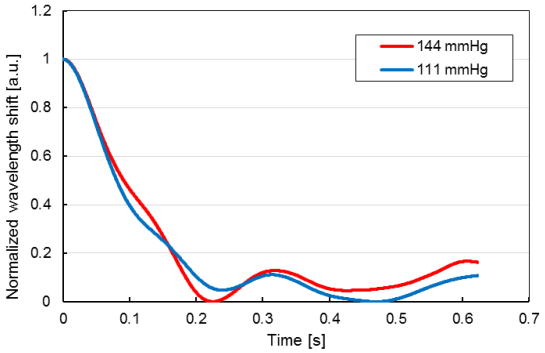

(e)

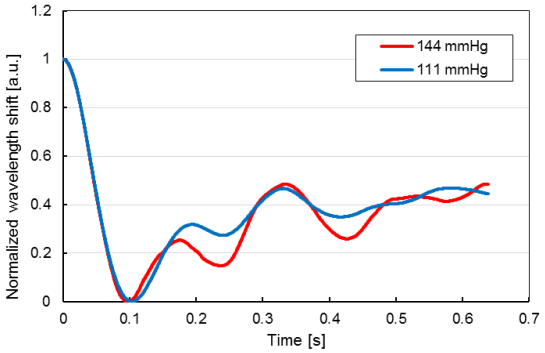

(f)

Figure 3-6. Left panels: Pulse waves without the differential processing for: (a) Subject A; (c) Subject B; (e) Subject C; Right panels: Pulse waves after the differential processing for: (b) Subject A; (d) Subject B; (f) Subject C

3.5. Blood Pressure Value Prediction Using Pulse Wave Signals Measured by FBG Sensor

The results of the blood pressure values (SBP and DBP) predicted using the pulse wave signals described in the previous section for each subject are shown in Figure 3-7.

In the prediction of SBP values, the standard errors (SE) for subjects A, B, and C were 3.2, 3.5, and 2.5 mmHg, respectively. The measurement error of the proposed measurement system is enough small because the measurement accuracy of conventional blood pressure measurement device is approximately 5 mmHg. Additionally, the correlation coefficients (R) were 0.93, 0.70 and 0.98 respectively, and they are significantly large for all the subjects. The results obtained for subject B were relatively less correlated with the reference values compared with that of the other subjects. As shown in Figure 3-5, the range of reference SBP values for subject B were narrower than those for the other subjects. Additionally, the shape change of the pulse wave signal measured by the FBG sensor for subject B was smaller than the changes observed for other subjects (Figure 3-6). Therefore, the calibration model constructed by the PLSR method for subject B does not represent the pulse wave shape change measured by the FBG sensor associated with the blood pressure change.

The SE in prediction of the DBP values for subjects A, B, and C were 3.4, 3.0, and 1.6 mmHg, respectively. These error values were also small as the SBP error values. The correlation coefficients for the DBP values were 0.95, 0.91 and 0.98 respectively and they are larger and better than those of the SBP values. As evidenced from the reference and the predicted DBP values in the second to

fourth measurement for the subjects A and B shown in Figure 3-7, the change in the reference DBP value was greater than 10 mmHg, whereas the predicted DBP values hardly changed in these measurements. The consistency in the predicted DBP values was observed due to the averaging of the pulse wave signal measured by the FBG sensor. The pulse wave signal used for blood pressure value prediction was averaged over approximately 30 pulse signals measured by the FBG sensor. Even though the shape of each pulse wave signal is different, each reference blood pressure value was measured in approximately 30 seconds. Therefore, the pulse wave signal used for calculating the predicted blood pressure value was averaged with respect to the measurement time of approximately 30 seconds. By averaging the pulse wave signals, the change in the shape of the pulse wave signal became gradual, although the reference blood pressure values changed suddenly. As a result, the difference between the shape of the pulse waves before and after the sudden change in the blood pressure is insignificant, and the predicted blood pressure values did not change significantly.

The FBG sensor measures the strain on the skin surface due to the volume change of the artery. Moreover, the strain in the skin surface changes with the pressure exerted by the blood flowing in the blood vessel. In other words, the pulse wave signal measured by the FBG sensor carries the information of the blood flow and flexibility of the blood vessel, and these parameters are affected by a change in the blood pressure values. Therefore, I infer that the pulse wave signal measured by the FBG sensor system has enough information to accurately predict the blood pressure values. Furthermore, the differences in the body

structure of individuals such as the thickness of the blood vessels, skin, and tissues can also affect the strain measured at the skin surface, which may affect the accuracy of the blood pressure measurements with this system. Considering the impact of the subject-based differences, it is important to reconsider the signal process to emphasize the shape change by blood pressure change for accurate prediction.

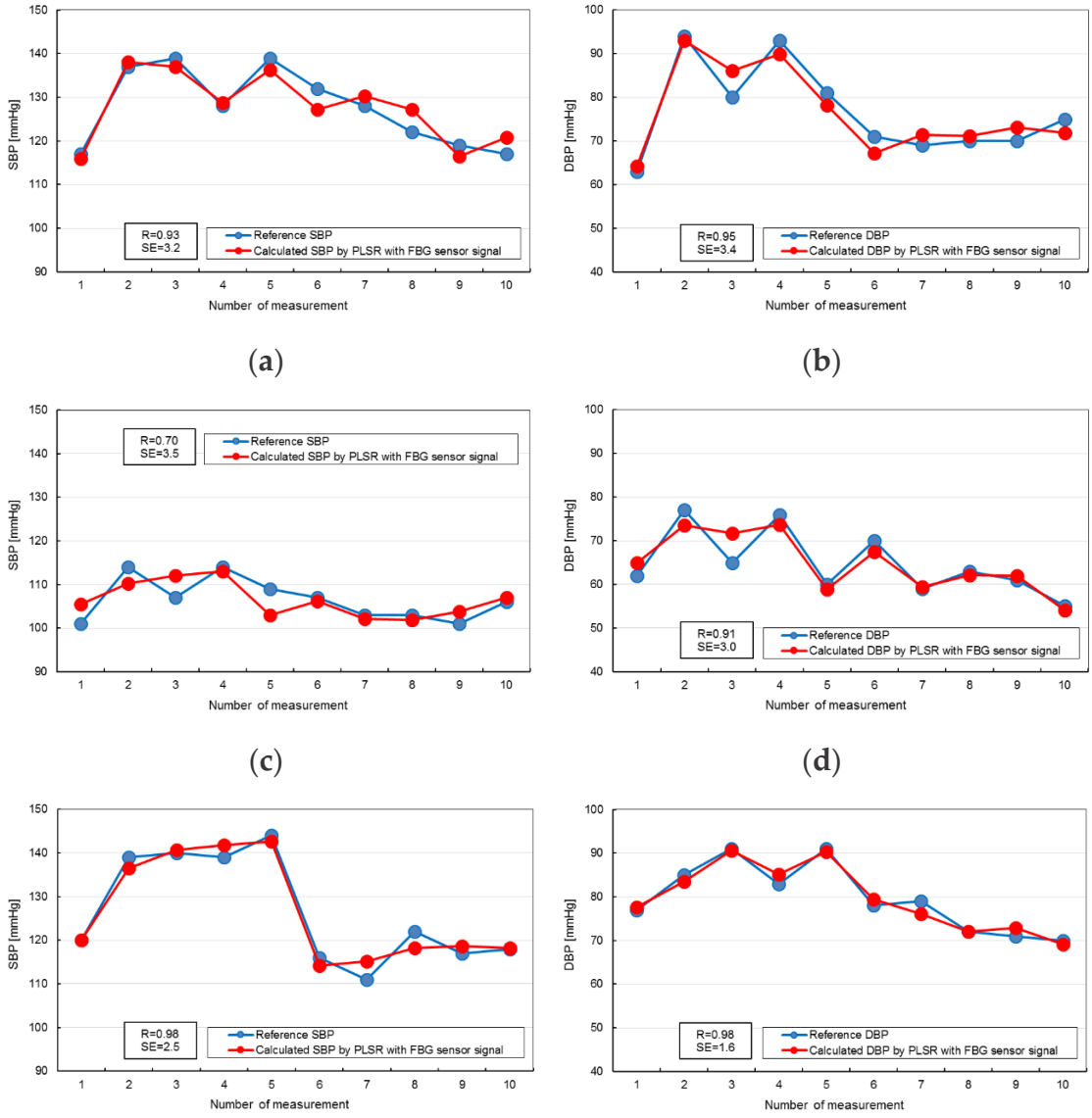

Figure 3-7. Left panels: Results of SBP predictions for: (a) Subject A, (b) Subject B, (c) Subject C; Right panels: Results of DBP predictions for: (a) Subject A, (b) Subject B, and (c) Subject C

3.6. Conclusion

An FBG sensor-based blood pressure prediction system for smart textile is proposed. In this work, I have demonstrated the use of the proposed system for predicting the sudden changes in the blood pressure values as observed in real-life situations. The validation that our system can trace sudden blood pressure change is essential to realize the wearable and continuous blood pressure monitoring system. Our previous studies showed that this system can efficiently measure the gradually changing blood pressures values. The proposed measurement system utilizes the changes measured in the pulse wave signals by the FBG sensor to predict the changes in the blood pressure values. The sudden change in the blood pressure was simulated by the cold pressor test. I observed a variation in the blood pressure values for different subjects owing to the difference in the rise of sympathetic nerve activity. The signal processing performed in this chapter can efficiently emphasize the shape change of the pulse wave signals. The shape of the pulse waves reflected from the peripheral blood vessels were remarkably different, when the reference blood pressure value was high compared with the low blood pressure. The results indicate that the proposed FBG sensor-based system was able to trace accurately the sudden changes in the blood pressure without delay; hence, it can be used as a blood pressure measuring device. However, I need to note that the shape change of pulse wave signal with blood pressure value change has individual difference. That means some subject's pulse wave shape changes greatly with the blood pressure value change, other subject's hardly changes. Therefore, it is necessary to reconsider the signal process to emphasize the shape change by blood pressure

change. Moreover, the placement of the FBG on the skin surface may affect the signal; therefore, it is necessary to establish a method to resolve such issues. Furthermore, for realizing a continuous measurement and for solving the problem that the change in the shape of the pulse wave signal became gradual by averaging, the measurement of reference values continuously using a blood pressure measurement device which takes shorter than 30 s for each measurement is a requisite.

Owing to the fibrous shape of FBG sensor, it can be inserted into the wearable textile materials for blood pressure measurements. The continuous monitoring of blood pressure may help in early detection and prevention of diseases. Moreover, we have already reported that other vital signs such as heart rate, respiration rate, and blood glucose can be measured by the FBG sensor. Hence, combining these vital sign measurement systems with the proposed blood pressure measurement system into a single FBG sensor-based system may be useful as a reliable method for an extensive and continuous monitoring of health.

3.7. References

[3-1] “Population Estimates, Current Population Estimates as of October 1, 2018,” Statistics Bureau. [Online]. Available: https://www.stat.go.jp/english/data/jinsui/2018np/index.html#header. [Accessed: 02-Nov-2019].

[3-2] “Population Projections for Japan: 2016 to 2065,” National Institute of Population and Social Security Research. [Online]. Available: http://www.ipss.go.jp/pp-zenkoku/e/zenkoku_e2017/pp_zenkoku2017e.asp. [Accessed: 02-Nov-2019].

[3-3] “Annual Report on the Aging Society: 2015 (Summary),” Cabinet Office, Government of Japan. [Online]. Available: https://www8.cao.go.jp/kourei/english/annualreport/2015/2015pdf_e.html.

[3-4] “2014 Summary of Patient Survey,” Ministry of Health, Labour and Welfare. [Online]. Available: https://www.mhlw.go.jp/english/database/db-hss/sps_2014.html. [Accessed: 01-Nov-2019].

[3-5] “Estimates of National Medical Care Expenditure, FY 2015,” Ministry of Health, Labour and Welfare. [Online]. Available: https://www.mhlw.go.jp/toukei/saikin/hw/k-iryohi/15/index.html. [Accessed: 01-Nov-2019].

[3-6] M. Rothmaier, B. Selm, S. Spichtig, D. Haensse, and M. Wolf, “Photonic textiles for pulse oximetry,” Optics Express, vol. 16, pp. 12973–12986, 2018.

[3-7] J. Witt et al., “Medical Textiles With Embedded Fiber Optic Sensors for Monitoring of Respiratory Movement,” IEEE Sens. J., vol. 12, no. 1, pp. 246–254, Jan. 2012, doi: 10.1109/JSEN.2011.2158416.

[3-8] A. Grillet et al., “Optical Fiber Sensors Embedded Into Medical Textiles for Healthcare Monitoring,” IEEE Sens. J., vol. 8, no. 7, pp. 1215–1222, Jul. 2008, doi: 10.1109/JSEN.2008.926518.

[3-9] Y. Miyauchi, H. Ishizawa, and M. Niimura, “Measurement of Pulse Rate and Respiration Rate Using Fiber Bragg Grating Sensor,” Trans. Soc. Instrum. Control Eng., vol. 49, no. 12, pp. 1101–1105, 2013, doi: 10.9746/sicetr.49.1101.

[3-10] S. Sato, M. Kawamura, Y. Miyauchi, and H. Ishizawa, “Simultaneous measurement of the pulse rate and respiratory rate by fiber Bragg grating sensors,” presented at the 28th SICE Sensing Forum, Yokohama, Japan, 2011, pp. 97–100.

[3-11] Y. Miyauchi, H. Ishizawa, S. Sato, and A. Hattori, “Development of the pulse rate measuring system by FBG sensors,” presented at the 10th JSMBE Symposium Nagano district, Nagano, Japan, 2012, pp. 13–14.

[3-12] Y. Katsuragawa and H. Ishizawa, “Non-invasive blood pressure measurement by pulse wave analysis using FBG sensor,” presented at the 2015 IEEE International Instrument and Measurement Technology Conference (I2MTC), Pisa, Italy, 2015, pp. 511–515, doi: 10.1109/I2MTC.2015.7151320.

[3-13] S. Chino, H. Ishizawa, S. Hosoya, S. Koyama, and K. Fujimoto, “Non-invasive blood pressure measurement—The study of measuring points,” presented at the SICE Annual Conference 2016, Tsukuba, Japan, 2016, pp. 1706–1709, doi: 10.3390/s17010048.

[3-14] S. Koyama, H. Ishizawa, K. Fujimoto, S. Chino, and Y. Kobayashi, “Influence of Individual Differences on the Calculation Method for FBG-

Type Blood Pressure Sensors," Sensors, vol. 17, no. 1, Dec. 2016, doi: 10.3390/s17010048.

[3-15] S. Koyama, A. Sakaguchi, H. Ishizawa, Y. Kurumi, H. Oshiro, and H. Kimura, "Vital Sign Measurement Using Covered FBG Sensor Embedded into Knitted Fabric for Smart Textile," J. Fiber Sci. Technol., vol. 73, no. 11, pp. 300–308, 2017, doi: 10.2115/fiberst.2017-0046.

[3-16] A. Sakaguchi, M. Kato, H. Ishizawa, H. Kimura, and S. Koyama, "Fabrication of Optical Fiber Embedded Knitted Fabrics for Smart Textiles," J. Text. Eng., vol. 62, no. 6, pp. 129–134, 2016, doi: 10.4188/jte.62.129.

[3-17] Y. Sano and T. Yoshino, "Fast optical wavelength interrogator employing arrayed waveguide grating for distributed fiber Bragg grating sensors," J. Light. Technol., vol. 21, no. 1, pp. 132–139, Jan. 2003, doi: 10.1109/JLT.2003.808620.

[3-18] Y. Sano and T. Yoshino, "Effect of light source spectral modulation on wavelength interrogation in fiber Bragg grating sensors and its reduction," IEEE Sens. J., vol. 3, no. 1, pp. 44–49, Feb. 2003, doi: 10.1109/JSEN.2003.809027.

[3-19] M. Todd, G. A. Johnson, and C.-C. Chang, "Passive, light intensity-independent interferometric method for fibre Bragg grating interrogation," Electron. Lett., vol. 35, pp. 1970–1971, Nov. 1999, doi: 10.1049/el:19991328.

[3-20] H. Martens and T. Næs, Multivariate Calibration. John Wiley & Sons, 1992.

[3-21] S. Hinohara and S. Okada, How to see and read the vital signs. Shorinsha, 2004.

[3-22] Y. Miyauchi, S. Koyama, and H. Ishizawa, "Basic experiment of blood-

pressure measurement which uses FBG sensors," presented at the 2013 IEEE International Instrumentation and Measurement Technology Conference (I2MTC), Minneapolis, MN, USA, 2013, pp. 1767–1770, doi: 10.1109/i2mtc.2015.7151320.

[3-23] E. A. Hines and G. E. Brown, "The cold pressor test for measuring the reactibility of the blood pressure: Data concerning 571 normal and hypertensive subjects," Am. Heart J., vol. 11, no. 1, pp. 1–9, Jan. 1936, doi: 10.1016/S0002-8703(36)90370-8.

Chapter 4

Improvement of Blood Pressure Prediction Using Artificial Neural Network

4.1. Introduction

With the rapid progression of the aging population, high medical expenses become a problem. Especially, the medical expense for patients with high blood pressure is over 1.8 trillion yen and the number of the patients is over 10 million [4-1], [4-2]. The high blood pressure is one of the risk factors for cardiac diseases such as heart attack and cerebral infarction. Moreover, the blood pressure changes easily according to both physical and mental states all day. Therefore, the daily base health monitoring is important and the home monitoring device which can measure continuously has been demanded. However, the continuous measurement is difficult with conventional measuring devices. Furthermore, the devices not only give physical stress caused by a cuff, but also they are inconvenient for carrying [4-3].

I have attempted to develop a wearable blood pressure measurement device using a Fiber Bragg Grating (FBG) sensor replacing conventional devices that could measure continuously, non-invasive and unconstrained. The FBG sensor is a thin optical fiber type strain sensor which has high sensitivity and high precision. Thanks to the sensor shape, the sensor can be inserted into the fabric easily and doesn't give physical stress to the user. Moreover, the sensor can be used in a special environment such as magnetic resonance imaging room since it is not affected by electromagnetic noise. Accordingly, the FBG sensor is suitable to develop the continuous, non-invasive and unconstrained blood pressure measurement device.

In the previous studies, the usefulness of the FBG sensor to various vital sign measurements such as respiration rate and stress was shown [4-4]–[4-8]. By

attaching an FBG sensor on the pulsation point, it can detect a slight change of expansion and contraction of the artery, namely the pulse wave. For the blood pressure prediction, the blood pressure was calculated by calibration curve constructed with Partial Least Squares Regression (PLSR) using the pulse waves obtained by the FBG sensor. The prediction accuracy is high enough when using the calibration curve constructed by the pulse waves of an individual or several people in their 20s [4-9]. However, it is not clear that the calibration curve constructed by the pulse waves obtained by a wide age group can predict the blood pressure correctly.

In this chapter, the number of subjects was increased and expand the age group of subjects. Then, the blood pressure was calculated both with PLSR and Artificial Neural Network (ANN). Finally, I compared the prediction accuracy of two prediction methods. Consequently, I found ANN was better prediction method since the effect of individual difference was lower.

4.2. Measurement Principle

4.2.1.Principle of the FBG sensor system

In this experiment, I used an FBG sensor system (PF25-S01: Nagano Keiki, Inc., Tokyo, Japan), same as in chapter 2 and 3. Figure 4-1 shows the optical system of an FBG sensor system and Figure 4-2 shows the schematic view of the sensor part. This system consists of an interrogator and an optical fiber. The wavelength range of Amplified Spontaneous Emission (ASE) light source is 1528-1570 nm and the output power is 20 mW. The diffraction grating in which the high and low refractive index part are arranged alternately at a constant period is formed in a part of the optical fiber core. A broadband infrared light is emitted from the ASE light source and only a specific wavelength which satisfies a formula (1) is reflected in the diffraction grating part:

$$\lambda_B = 2n_{eff.}\Lambda \qquad (1)$$

where λ_B is the Bragg wavelength, $n_{eff.}$ is the refractive index of the gating part, and Λ is the diffraction grating spacing. When the diffraction grating interval is changed by pressure, the Bragg wavelength also changes according to the formula (1). The Bragg wavelength shift is detected by the Mach-Zehender interferometer. Finally, the strain change of the sensor part is calculated with this wavelength shift [4-10], [4-11]. The resolution of the wavelength shift is 0.1 pm, the resolution of the distortion is 0.08 μ strain in this system [4-12]. This high strain measuring system enables us to detect the slight change of expansion and contraction propagated from the blood vessel.

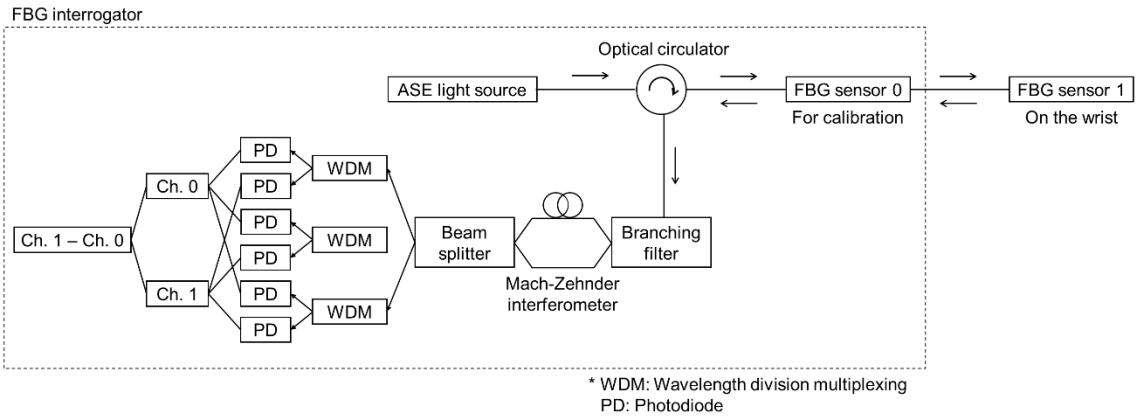

Figure 4-1. The optical system of an FBG sensor system

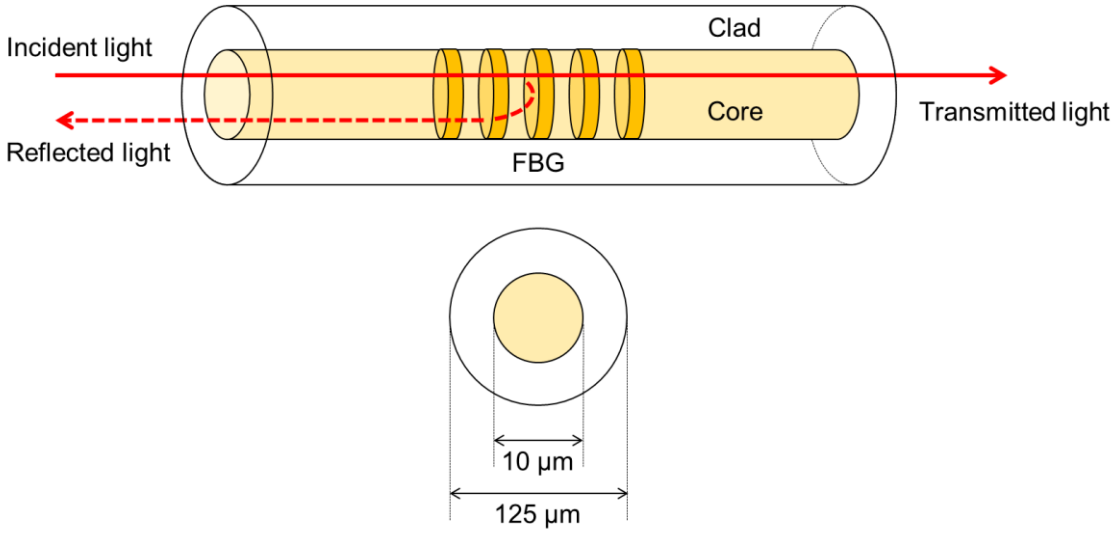

Figure 4-2. The schematic view of the sensor part

4.2.2.Partial Least Squares Regression (PLSR)

PLSR is an analytical method which predicts the objective variables from the relation between the objective variables and the explanatory variables. In PLSR, the principal component factor called PLS factor is calculated using an explanatory variable and an objective variable which are assumed to include an error and the regression equation is built. Then, a new objective variables are

calculated with the regression equation. With this new objective variables and the explanatory variables, a new PLS factor is calculated. A new regression equation and new objective variables are recalculated by adding the new PLS factor. Repeating this progress, and increasing the number of PLS factor, a regression equation which makes small error is calculated. The optimum number of PLS factor is verified by leave-one-out method when the new PLS factor is calculated. By the F-test, the prediction residual error sum of squares (PRESS) of PLS model before and after adding PLS factor are compared. PLS factor is added if the difference between the PRESS of both PLS model is significant. On the other hand, if the difference is not significant, the regression equation of the model with a smaller number of PLS factor is selected as the calibration curve.

In this chapter, the PLSR was used for the calibration curve construction since the referenced blood pressure values measured by the blood pressure pulse wave inspection apparatus include an error. In this chapter, the pulse waves measured by the FBG sensor are used as the explanatory variables and reference blood pressure values are used as the objective variables for the calibration curve construction. Then, in order to calculate the blood pressure, the pulse waves of the subjects measured by the FBG sensor are substituted into the calibration curve.

4.2.3.Artificial Neural Network (ANN)

ANN is a computing analyzing method inspired by the biological neural networks that constitute animal brains. In ANN, data processing performed by nerve cells is replaced by processing elements called units and information

processing is performed by combining each unit. In this chapter, to calculate blood pressure, using the nonlinear unit, I constructed a feedforward neural network in which data processing proceeds in one direction. The network learning is supervised and the layer structure is three layers of the input layer, the hidden layer, and the output layer. In this chapter, the number of sampling point was adjusted in 6011. Therefore, the number of the input layer is 6011 which corresponds to the number of sampling point. The one of the hidden units is 500 to avoid over-learning and the one of the output layer is 1, or the prediction blood pressure. The feedforward neural network having one output unit performs nonlinear modeling on the relationship between multivariate explanatory variables and objective variables. Using the backpropagation, the combined load and the bias of the network are adjusted in order to reduce the output error. The sigmoid function is used to calculate the output value of each unit [4-13]. The learning rate is 0.1, the decrease coefficient is 0.9, the increase coefficient is 1.03, and Momentum coefficient is 0.85.

4.3. Experimental Methods

Pulse waves can be measured at several points on the surface of human body such as the wrist and neck [4-14]. We found that the pulse wave was able to be measured at these points using FBG sensor in previous studies [4-4]–[4-8]. In this chapter, FBG sensor was fixed on the surface of the left wrist using medical tape as shown in Figure 4-3 and the pulse waves were measured.

The subjects were 77 persons whose age ranged from 21 to 87. 44 of them were male and the other 33 were female. The measurement position was the supine position. The reference blood pressure was measured simultaneously at the right upper arm with the blood pressure pulse wave inspection apparatus (VS-1500N: FUKUDA DENSHI). The measurement error is less than ∓3 mmHg. The measurement time with FBG sensor was about 30 seconds in accordance with the measurement time of the apparatus. The sampling frequency was 10 kHz. The number of the measurement for each subject was once or twice due to the subject's condition, time limitation or fails of data acquisition. The data obtained in this chapter were 132 in total.

The measurement signal has background noise such as electromagnetic noise and thermal noise. Therefore, a band-pass filter was applied to the measured pulse waves to reduce the effects of noise. The passband was 0.5 to 5 Hz [4-4]–[4-8], [4-15]. Then, the filter-processed signal is divided at the peak. The divided signal corresponds to a single heartbeat. Then, the divided signals were averaged and normalized in measurement time. The height of the first point and the minimum point were normalized into 1 and 0. In addition, the number of sampling points was unified in the fewest number of samples. Finally, the blood

pressure was calculated with PLSR and ANN using the signal processed pulse waves and the reference blood pressure.

100 data were chosen randomly from the overall 132 data to construct the calibration curve or the network learning and the remaining 32 data were used for the validation. The data set used for PLSR and ANN was the same. In this chapter, I compared the results of PLSR with the ones of ANN in order to know which a better method for the blood pressure prediction was.

The protocol for this study was approved by the Ethics Committee of Shinshu University (Project identification code: No. 3202, Verification clinical trial with wearable vital sign measurement system).

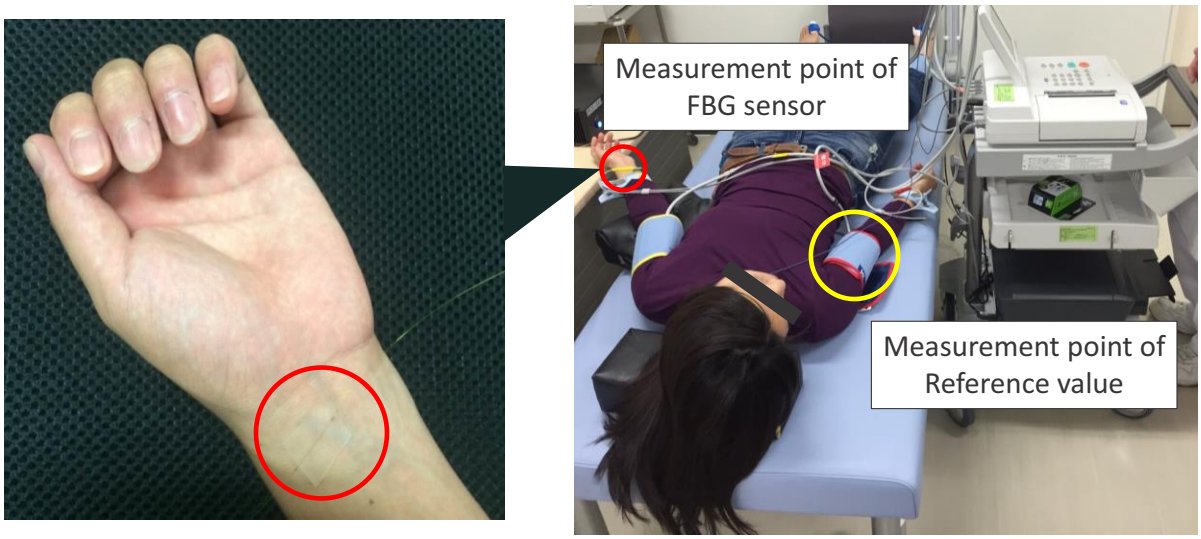

Figure 4-3. Measurement using the FBG sensor

4.4. Experimental results and discussion

The calibration/ network learning and validation data set used in this chapter are shown in Table 4-1. The calibration/ network learning data set was used to construct the calibration curve using PLSR or was used for the learning of ANN. The results of the calibration curve using PLSR are shown in Figure 4-4 and Table 4-2. From Table 4-2, the standard error of calibration (SEC) is 15 mmHg, and the standard error of prediction (SEP) is 18 mmHg when using the calibration curve constructed by PLSR. Considering the measurement accuracy of the conventional blood pressure meter is about 5 mmHg, the blood pressure prediction with PLSR does not have sufficient accuracy. Moreover, many data have a large error and the correlation coefficient does not have high significance. Therefore, the reliability of the calibration curve is low.

Figure 4-5 shows the loading vectors of each factor which are used for calibration curve construction and one of the pulse waves which is measured in this chapter. The loading vector indicates the dependence of each factor on the calibration curve. The loading vector of Factor 1 is similar to the pulse wave signal. In the loading vector of Factor 2, 3, and 4, the biggest absolute values take at 0.28, 0.08, and 0.20 s respectively. These points correspond to the local maximum value point and local minimum value point of the pulse wave. Therefore, each factor affects the changing points of the pulse waveform. However, some data had a large error. Figure 4-6 shows the normalized pulse waves which were used for validation and had the same reference blood pressure. One of them had a small error (surrounded by the circle in Figure 4-4) and the other one had a large error (surrounded by the dashed circle in Figure 4-4). The shape of these pulse waves

is different, especially around 0.30 s. Therefore, the calibration curve constructed by PLSR was not possible to adapt enough to the change in the pulse wave shape well. In this chapter, the calibration curve was constructed with the data of multiple subjects. It means the pulse waves which should be classified into different pattern were used for the calibration curve construction. If the calibration curve is constructed for each subject described in chapter 3, the change in pulse wave shape with the change in blood pressure is detectable and the calibration curve constructed by PLSR is possible to adapt enough for the blood pressure estimation. However, if the calibration curve is constructed with the pulse wave signals which have a different pattern, the effect of the difference between patterns are big and it becomes difficult for the calibration curve constructed by PLSR to detect the change in pulse wave shape with the blood pressure change. That's why I used ANN for blood pressure prediction to adapt the shape change by fixing the number of the input unit to the number of data points.

Table 4-1. Calibration/ network learning and validation data set

	Samples	Min (mmHg)	Max (mmHg)	Avg. (mmHg)
Calibration	100	95	180	129
Validation	32	111	183	133

Table 4-2. Result of calibration curve using PLSR

Calibration	Factor	4
	Correlation coefficient	0.34
	Mean Error (mmHg)	0
	SEC(mmHg)	15
	Mean Absolute Error (mmHg)	12
Validation	Mean Error (mmHg)	-4
	SEP (mmHg)	18
	Mean Absolute Error (mmHg)	15

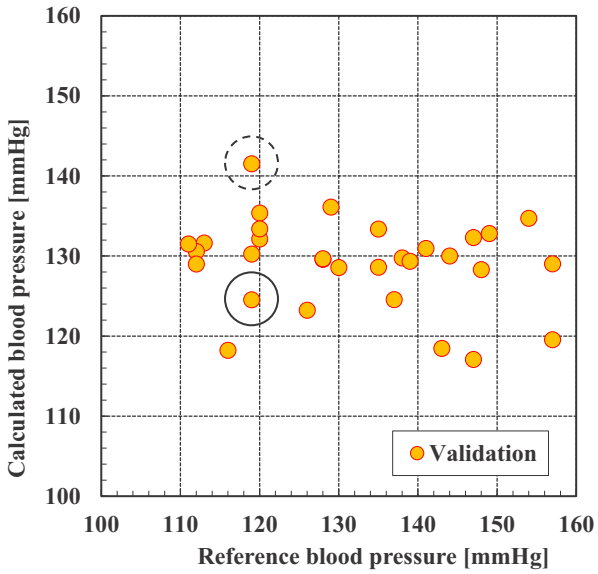

Figure 4-4. Result of calibration curve using PLSR

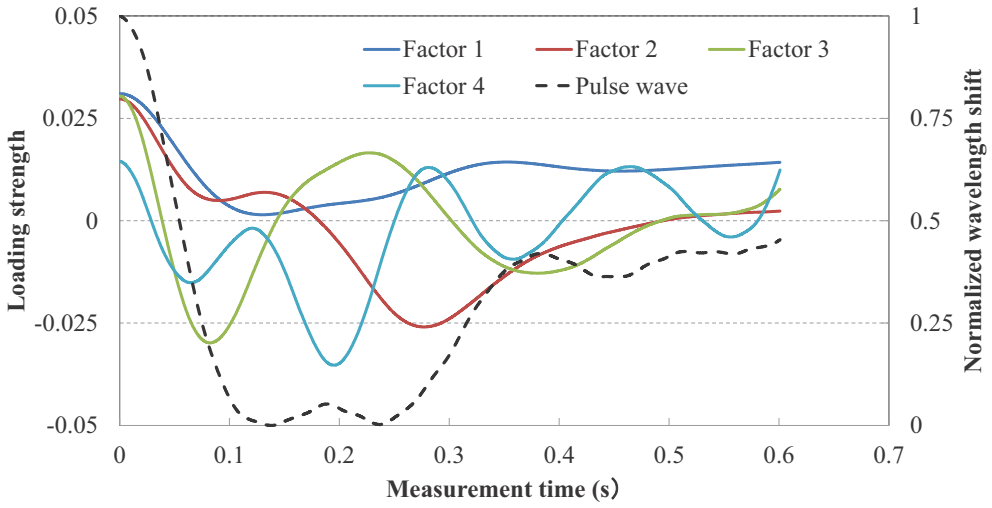

Figure 4-5. Loading vectors of the calibration curve and the pulse wave

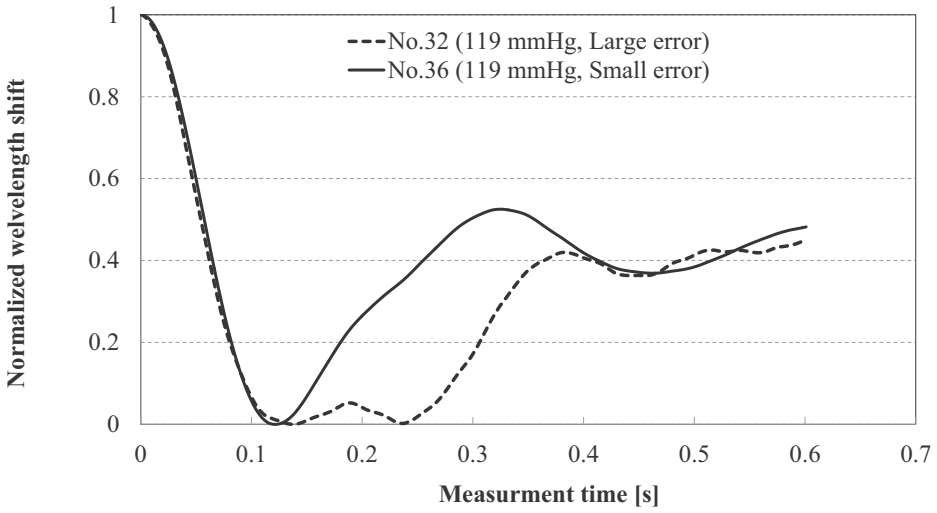

Figure 4-6. Normalized pulse waves which have a large error and a small error

Table 4-3 and Figure 4-7 show the result of ANN. The SEC and SEP are 9 mmHg and 17 mmHg respectively. Both of them become smaller than using the calibration curve constructed by PLSR, in other words, the prediction accuracy

becomes higher when using ANN. Furthermore, while the correlation efficient of the calibration curve using PLSR was 0.34, the one using ANN was 0.83 so that there was a significant correlation between the reference blood pressure and the calculated blood pressure. However, many data are not predicted well. Comparing with the measurement accuracy of the conventional blood pressure measuring device, the blood prediction accuracy of ANN is lower. The data surrounded by the circle and the dashed circle in Figure 4-7 are the same data surrounded by the circle and the dashed circle in Figure 4-5. The data which have low prediction accuracy with PLSR also tend to have a low prediction accuracy with ANN. The comparison of the normalized pulse waves for validation which have a large error and a small error with the one for the network learning is shown in Figure 4-8. These pulse waves have almost the same reference blood pressure. Between 0.1 to 0.4 s, the shape of the pulse wave for validation whose error is large differs greatly from the one for the network learning while the shape of the pulse wave for validation whose error is small is similar to the one for the network learning. Therefore, ANN used in this chapter calculated the blood pressure from the difference in the shape between 0.1 to 0.4 s. Thus, the individual difference of the pulse wave shape affected the prediction accuracy of ANN as well as the prediction with PLSR. According to Sano, et al, the human pulse wave can be classified into seven patterns A-G depending on age and whether the subject has the vascular disease [4-16]. Classifying the pulse waves into the patterns, the effect of individual difference may be eliminated. It is also necessary to reconsider the number of hidden layer unit and the learning parameters to get higher prediction accuracy. Consequently, the effect of

individual difference could be reduced by using ANN and it is suitable to use ANN for the blood pressure prediction. In the next chapter, focusing on the individual difference, the verification whether the classification of pulse wave signal pattern is effective for improving the blood pressure value estimation.

Table 3. Result of ANN

Calibration	Correlation coefficient	0.83
	Mean Error (mmHg)	0
	SEP (mmHg)	9
	Mean Absolute Error (mmHg)	6
Validation	Mean Error (mmHg)	0
	SEC (mmHg)	17
	Mean Absolute Error (mmHg)	12

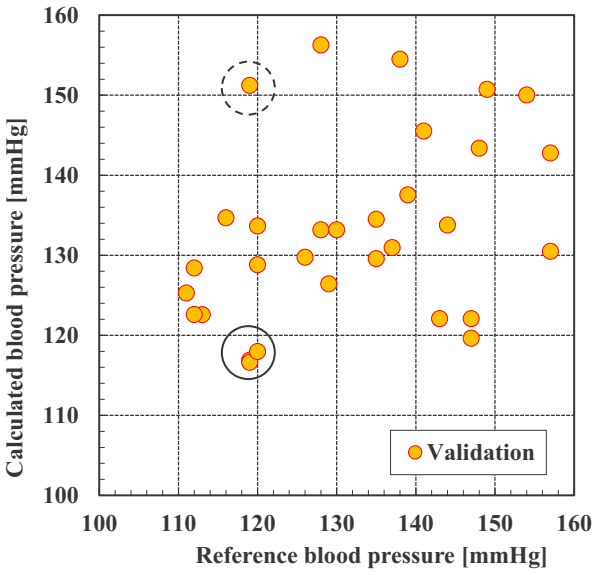

Figure 4-7. Result of ANN

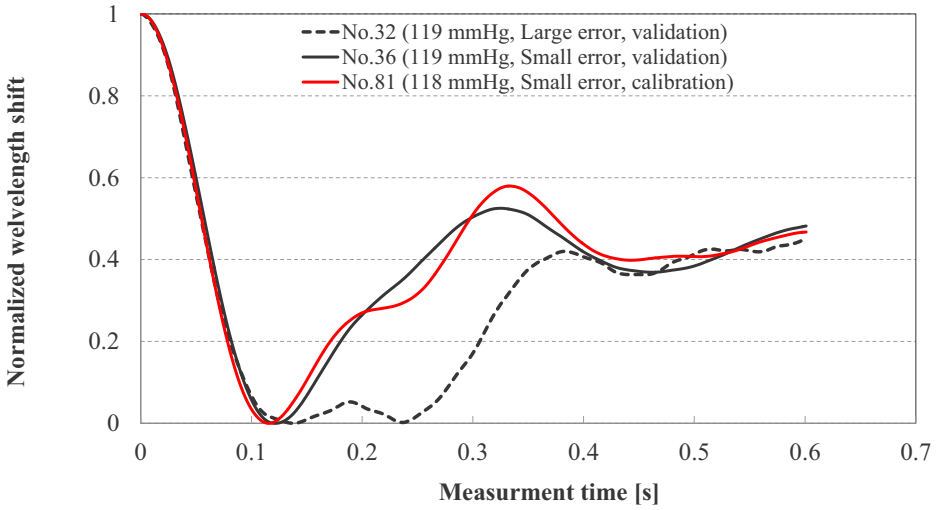

Figure 4-8. Comparison of the normalized pulse waves for validation which have a large error and a small error with the one for the network learning

4.5. Conclusion

In this chapter, I increased the number of the subjects, expand the age range of subjects to know whether the calibration curve constructed with the pulse waves of the wide age group can predict the blood pressure correctly. The pulse wave was measured by the FBG sensor and the blood pressure was predicted by two methods, PLSR and ANN. Then, comparing both results, I found which method was suitable for blood pressure prediction toward to the high versatility. The prediction accuracy of PLSR was low. Those are because the influence of the individual difference of the pulse wave shape was too big although each factor affects the pulse waveform changing points. Moreover, the correlation coefficient was so small. Therefore, the reliability of the calibration curve constructed by PLSR was not high enough. On the other hand, using ANN for the blood pressure prediction, it was possible to get higher prediction accuracy and bigger correlation coefficient than using PLSR. Although the blood pressure prediction with ANN is affected by the individual difference of the pulse waveform as well as PLSR, the optimization of the combined load and the bias of the network by the repetitive learning could reduce the effect of the individual difference. Consequently, the blood pressure prediction method for the versatile use, it is suitable to use ANN for the blood pressure prediction. However, it is not possible to eliminate the effect completely in this chapter. In the next chapter, I classify the pulse wave into seven patterns to eliminate the effect. It is also necessary to reconsider the number of hidden layer unit and the learning parameters to get higher prediction accuracy.

4.6. References

[4-1] “2014 Summary of Patient Survey,” Ministry of Health, Labour and Welfare. [Online]. Available: https://www.mhlw.go.jp/english/database/db-hss/sps_2014.html. [Accessed: 01-Nov-2019].

[4-2] “Estimates of National Medical Care Expenditure, FY 2015,” Ministry of Health, Labour and Welfare. [Online]. Available: https://www.mhlw.go.jp/toukei/saikin/hw/k-iryohi/15/index.html. [Accessed: 01-Nov-2019].

[4-3] K. Yamakoshi, “Progress of Non-invasive, Ambulatory, and Non-conscious Biomedical Measurement,” J. Jpn. Soc. Precis. Eng., vol. 62, no. 11, pp. 1525–1529, Jan. 1996.

[4-4] Y. Miyauchi, H. Ishizawa, and M. Niimura, “Measurement of Pulse Rate and Respiration Rate Using Fiber Bragg Grating Sensor,” Trans. Soc. Instrum. Control Eng., vol. 49, no. 12, pp. 1101–1105, 2013, doi: 10.9746/sicetr.49.1101.

[4-5] S. Sato, M. Kawamura, Y. Miyauchi, and H. Ishizawa, “Simultaneous measurement of the pulse rate and respiratory rate by fiber Bragg grating sensors,” presented at the 28th SICE Sensing Forum, Yokohama, Japan, 2011, pp. 97–100.

[4-6] Y. Miyauchi, H. Ishizawa, S. Sato, and A. Hattori, “Development of the pulse rate measuring system by FBG sensors,” presented at the 10th JSMBE Symposium Nagano district, Nagano, Japan, 2012, pp. 13–14.

[4-7] Y. Katsuragawa and H. Ishizawa, “Non-invasive blood pressure measurement by pulse wave analysis using FBG sensor,” presented at the 2015 IEEE International Instrument and Measurement Technology

Conference (I2MTC), Pisa, Italy, 2015, pp. 511–515, doi: 10.1109/I2MTC.2015.7151320.

[4-8] S. Chino, H. Ishizawa, S. Hosoya, S. Koyama, and K. Fujimoto, "Non-invasive blood pressure measurement—The study of measuring points," presented at the SICE Annual Conference 2016, Tsukuba, Japan, 2016, pp. 1706–1709, doi: 10.3390/s17010048.

[4-9] S. Koyama, H. Ishizawa, K. Fujimoto, S. Chino, and Y. Kobayashi, "Influence of Individual Differences on the Calculation Method for FBG-Type Blood Pressure Sensors," Sensors, vol. 17, no. 1, Dec. 2016, doi: 10.3390/s17010048.

[4-10] Y. Sano and T. Yoshino, "Fast optical wavelength interrogator employing arrayed waveguide grating for distributed fiber Bragg grating sensors," J. Light. Technol., vol. 21, no. 1, pp. 132–139, Jan. 2003, doi: 10.1109/JLT.2003.808620.

[4-11] Y. Sano and T. Yoshino, "Effect of light source spectral modulation on wavelength interrogation in fiber Bragg grating sensors and its reduction," IEEE Sens. J., vol. 3, no. 1, pp. 44–49, Feb. 2003, doi: 10.1109/JSEN.2003.809027.

[4-12] M. Todd, G. A. Johnson, and C.-C. Chang, "Passive, light intensity-independent interferometric method for fibre Bragg grating interrogation," Electron. Lett., vol. 35, pp. 1970–1971, Nov. 1999, doi: 10.1049/el:19991328.

[4-13] Yoshitomi Y., Neural network. Asakura Publishing Co., Ltd., 2002.

[4-14] S. Hinohara and S. Okada, How to see and read the vital signs. Shorinsha, 2004.

[4-15] Y. Miyauchi, S. Koyama, and H. Ishizawa, "Basic experiment of blood-

pressure measurement which uses FBG sensors," presented at the 2013 IEEE International Instrumentation and Measurement Technology Conference (I2MTC), Minneapolis, MN, USA, 2013, pp. 1767–1770, doi: 10.1109/i2mtc.2015.7151320.

[4-16] S. Yuji et al., "Evaluation of peripheral circulation with accelerated plethysmography and its practical application. | Article Information | J-GLOBAL," J Sci. Labor, vol. 61, no. 3, pp. 129–143, 1985.

Chapter 5

Validity of the Classification of Pulse Wave for the Blood Pressure Estimation

5.1. Introduction

The rate of ageing has been increasing globally in recent years and it is estimated to continue rising [5-1]. Under this circumstance, the development of a vital sign measuring device not only for elderly people but also for healthy people has been demanded [5-2], [5-3]. The vital signs are the heart rate, blood pressure (BP), body temperature, respiratory status, and the level of consciousness. These signs represent concisely the state of human health [5-4]. That means they change easily according to both physical and mental states. Therefore, it is desirable that the vital signs are measured continuously and the measuring device needs to be non-invasive and under physical unconstrained. However, conventional blood pressure measuring device has the physical constraint caused by the cuff and is not suitable for continuous measurement.

The aim of the research is to develop a wearable vital sign measurement sensor using a Fiber Bragg Grating (FBG) sensor that could measure them continuously in non-invasive and unconstrained, instead of conventional measuring devices. The FBG sensor is a small optical fiber type strain sensor and has high sensitivity and high precision. It is also inexpensive, has corrosion resistance and is not affected by electromagnetic noise. Therefore, this sensor can be used in a special environment such as magnetic resonance imaging (MRI) room. From the above reasons, this sensor is suitable for the continuous vital signs measurement.

In the previous studies, various vital signs measurement system using the FBG sensor has shown [5-5]–[5-9]. The FBG sensor can measure the distortion of the body surface. Thus, by detecting the expansion and contraction of the artery

it is possible to measure human pulse waves. With Partial Least Squares Regression (PLSR), a calibration curve was constructed and the blood pressure value was calculated. However, the optimal data set for constructing a calibration curve which is used to estimate blood pressure value has not been clarified yet. To realize the better blood pressure estimation method, it is necessary to find the optimal data set for constructing a calibration curve.

Sano et al reported that the human pulse wave can be classified into seven patterns A-G depending on age and whether the subject has vascular disease. Young, healthy people tend to have the pattern A or B, persons with high blood pressure tend to have the pattern C-G, and patients with a vascular disease such as cerebrovascular disease and ischemic heart disease tend to have the pattern E or F [5-10].

As mentioned in the previous chapter, the individual difference of pulse wave signals affect negatively on the estimation accuracy of blood pressure value. Therefore, in this chapter, I classified the pulse waves measured by the FBG sensor according to Sano's classification to construct calibration curves and calculated the blood pressure value. Comparing the calibration curve constructed with classified data and the one constructed with non-classified data, the effectiveness of the classification of pulse wave signal for the blood pressure value estimation was verified.

5.2. Measurement Principle

5.2.1.Principle of the FBG sensor system

I used an FBG sensor system in this experiment same as the chapters above. Figure 5-1 shows the optical system of an FBG sensor system and Figure 5-2 shows the schematic view of the sensor part. The diffraction grating is formed in a part of the optical fiber core. A broadband light is emitted from the light source, and the light reflected by the FBG sensor. The wavelength of the reflected light is called Bragg wavelength. When the diffraction grating interval is changed by pressure, the Bragg wavelength shifts. The Bragg wavelength is detected by the Mach-Zehender interferometer. Therefore, the wavelength shift corresponding to the strain change of the sensor part can be obtained [5-11], [5-12]. The resolution of the wavelength shift is 0.1 pm, the resolution of the distortion is 0.08 μ strain in this system [5-13]. This high strain measuring system enables to measure the pulse wave.

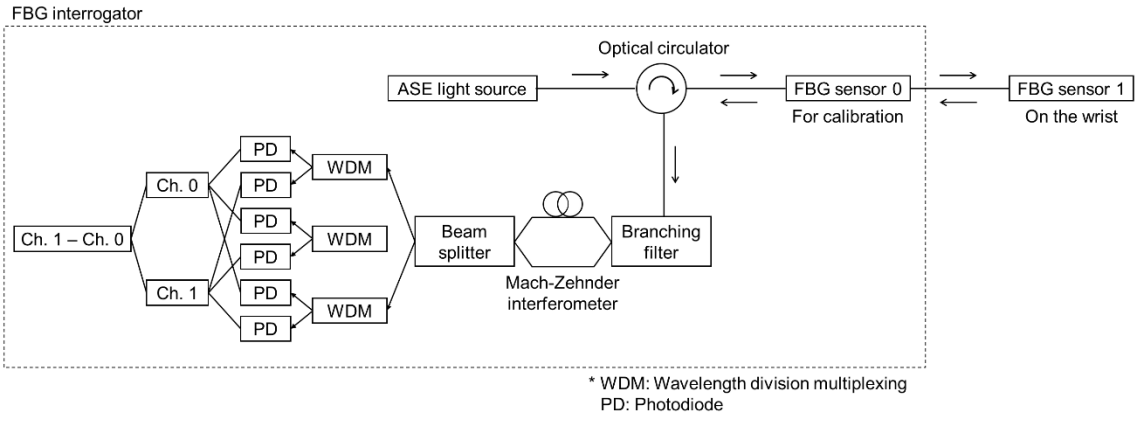

Figure 5-1. The optical system of an FBG sensor system

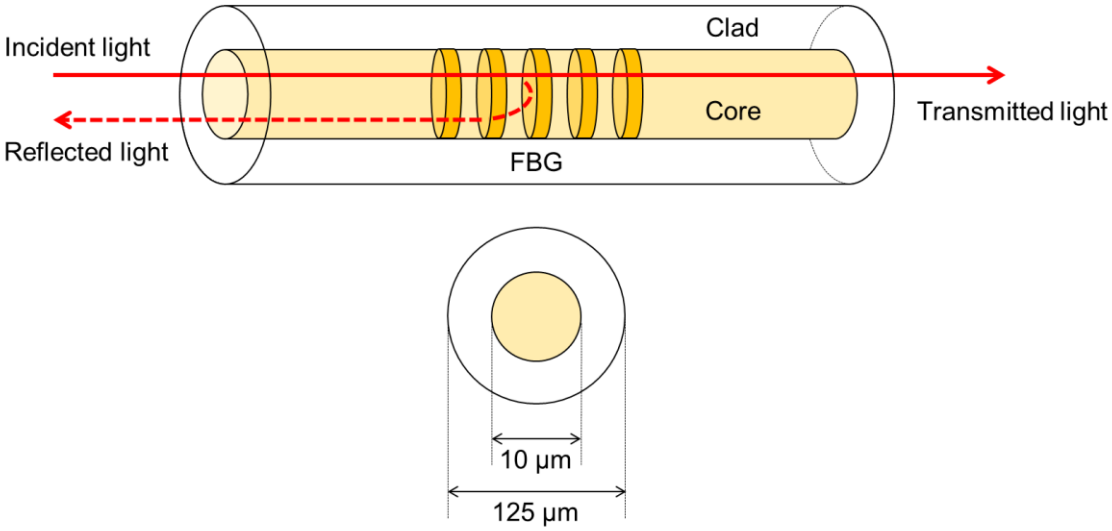

Figure 5-2. The schematic view of the sensor part

5.2.2.Partial Least Squares Regression (PLSR)

I calculated the blood pressure value using PLSR which is an analytical method of performing a regression analysis on principal component. This method assumes that both of an explanatory variable and an objective variable include an error. In this chapter, the pulse waves measured by the FBG sensor are used as the explanatory variables and reference blood pressure values are used as the objective variables. PLSR is used to construct the calibration curve since the referenced blood pressure values include an error. Then, measured pulse wave from subjects is substituted into the calibration curve to get predictive blood pressure.

5.3. Experimental Methods

Pulse waves can be measured at several points on the surface of the human body such as the wrist and temple [5-14]. The pulse wave is assumed to include information to calculate the blood pressure value since the pressure of the blood vessel due to the blood flow propagates to the surface of the body as a pulse wave. In this chapter, I fixed the FBG sensor on the surface of the left wrist using medical tape as shown in Figure 5-3 and measured the pulse waves. In the previous studies, we confirmed that the pulse wave was able to be measured at the wrist using FBG sensor [5-5]–[5-9].

The subjects were 77 persons. 44 of them were male and the other 33 were female. The age ranged from 21 to 87. The subjects were lying face-up during the measurement. The referenced blood pressure value was simultaneously measured at the right upper arm with the blood pressure pulse wave inspection apparatus (VS-1500N: FUKUDA DENSHI). The measurement time was about 30 seconds and the sampling frequency is 10 kHz. Each subject was measured once or twice due to the subject's condition, time limitation or fail of data acquisition, and 132 data were obtained in total. The data obtained in this chapter were classified by the same way as in chapter 4. The data were classified into 7 patterns (pattern A to G) as mentioned in chapter 2. The numbers of each pattern were shown in Table 5-1.

The measurement signal has background noise such as electromagnetic noise and thermal noise. I applied a band-pass filter to the measured pulse waves to reduce the effects of noise. The pass frequency is 0.5 to 5.0 Hz [5-5]–[5-9], [5-15]. This pass frequency band was chosen since the average pulse rate of the

general adult is 60 beats per minute (bpm). In order to obtain pulse waves corresponding to a single heartbeat, I spattered the filter processed signal into one cycle from one peak to the next peak. Then, the separated signals were averaged and normalized in measurement time. The height of the first point was 1, and the minimum point was 0 in the normalized signal. In addition, the number of sampling points was adjusted with the fewest number of samples. Then, I calculated blood pressure value. The calibration curve was constructed using PLSR. The explanatory and objective variables were the normalized signal and the referenced blood pressure value respectively.

To confirm how much the accuracy of blood pressure estimation changes by the classification of pulse wave signal measured by FBG sensor, the two data set were determined. The one data set was the classified data set. 40 data from 51 data of pattern A were used to construct the calibration curve and the remaining 11 data were used for validation. The other data set was the non-classified data set. The same 11 data as the classified data set were chosen as the validation data set, and the calibration curve was constructed with 40 data chosen from the remaining 121 data. Then, I compared the estimation results using the classified data with the ones using the non-classified data.

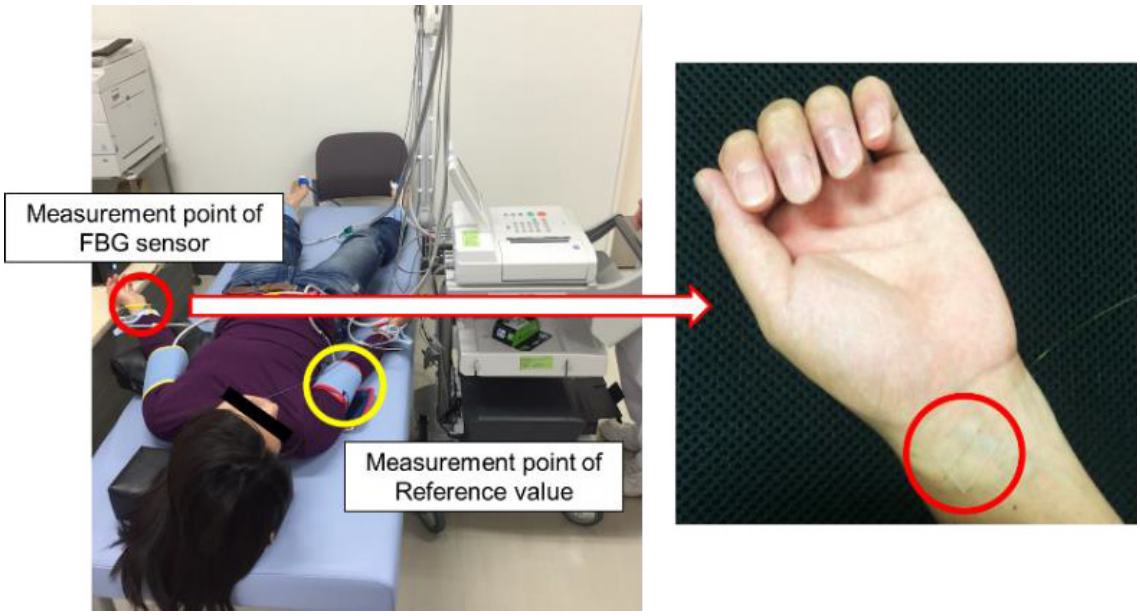

Figure 5-3. Experimental image of measurement using the FBG sensor

Table 5-1. Pattern classification results of pulse wave signal measured by the FBG sensor

	Pattern							
	A	B	C	D	E	F	G	Total
Number	51	19	13	15	4	12	18	132

5.4. Experimental Results and Discussion

5.4.1. Blood pressure value estimation results using non-classified data set

The calibration and validation results by PLSR with non-classified data set are shown in Figure 5-4 and Table 5-2. From Figure 5-4 (a) and Table 5-2 (a), the correlation coefficient of the SBP was 0.35, the standard error of calibration (SEC) was 18 mmHg and the standard error of prediction (SEP) was 22 mm Hg. From Figure 5-4 (b) and Table 5-2 (b), the correlation coefficient of the diastolic blood pressure (DBP) was 0.35, the SEC and SEP were 9 and 12 mmHg respectively. The correlation coefficient did not have high significance and the accuracy of blood pressure value estimation was low for both the SBP and DBP. As mentioned in the introduction, each subject has a different pattern of the pulse wave (Figure 5-5). In other words, the pulse wave shapes are quite different despite the referenced blood pressure value is the same. Furthermore, as Figure 5-6 shows, some pulse waves have two downward peaks. Therefore, the minimum point of the normalization shifted every pulse wave signal. Consequently, the coefficient correlation was small and the accuracy of blood pressure estimation was low.

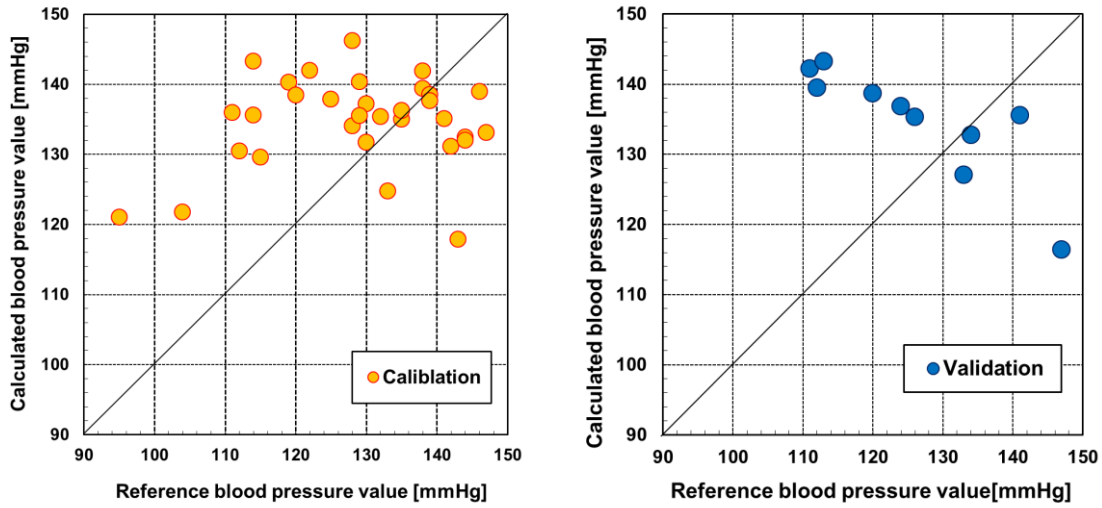

(a) SBP

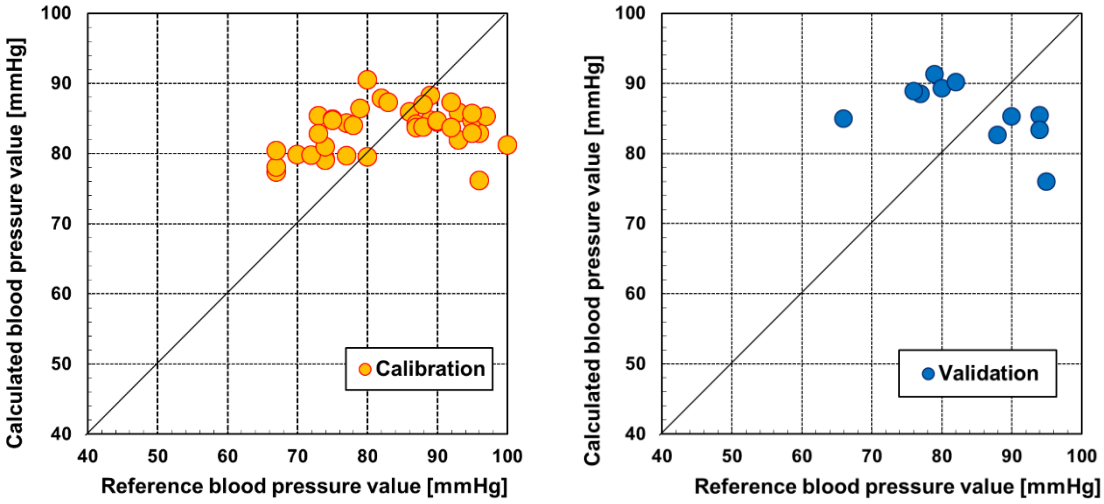

(b) DBP

Figure 5-4. Calibration curve and validation results using non-classified data set

Table 5-2. Calibration and validation results using non-classified data set

(a) SBP

Calibration			
Sample	Avg. [mmHg]	Min [mmHg]	Max [mmHg]
40	136	95	183
Result	Factor		4
	Correlation coefficient		0.35
	SEC [mmHg]		18

Validation			
Sample	Avg. [mmHg]	Min [mmHg]	Max [mmHg]
11	129	111	163
Result	SEC [mmHg]		22

(b) DBP

Calibration			
Sample	Avg. [mmHg]	Min [mmHg]	Max [mmHg]
40	83	67	100
Result	Factor		4
	Correlation coefficient		0.35
	SEC [mmHg]		9

Validation			
Sample	Avg. [mmHg]	Min [mmHg]	Max [mmHg]
11	84	66	95
Result	SEC [mmHg]		12

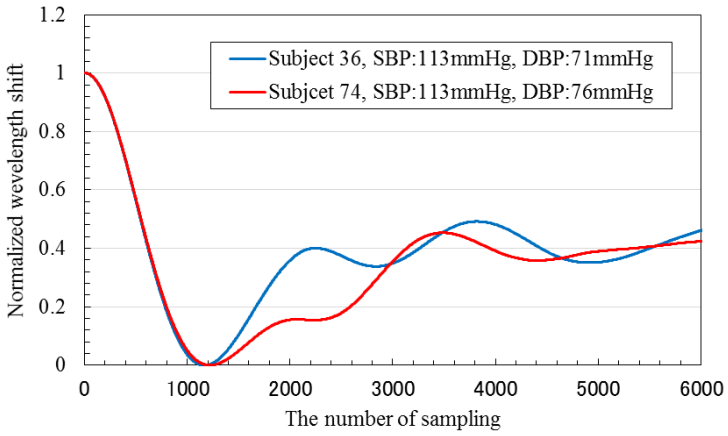

Figure 5-5. Normalized pulse waves which have the same referenced BP in SBP

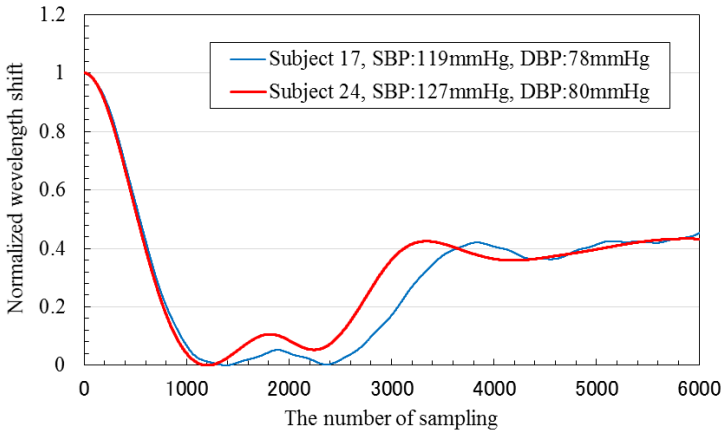

Figure 5-6. Normalized pulse waves which have two downward peaks

5.4.2. Blood pressure estimation results using the data classified into pattern A

In section 5.4.1, the accuracy of the blood pressure estimation using non-classified data set was low due to the individual difference of pulse wave shapes. Therefore, I calculated the blood pressure value with calibration curve constructed with the data classified pattern A. The pulse wave of subject 36 is

pattern A as Figure 5-5 shows. Pattern A has only one downward peak, thus, the minimum point was unified in the normalization. Figure 5-7 and Table 5-2 show the calibration and validation results using classified data set. The correlation coefficient of the SBP was 0.43, SEC and SEP were respectively 14 and 21 mmHg. The correlation coefficient of DBP was 0.60. SEC and SEP were 8 and 13 mmHg respectively. Comparing the results using non-classified data, the correlation coefficient tended to become big and SEC and SEP tended to be small by the pulse wave classification. Therefore, the possibility that the pulse wave classification improves the accuracy of blood pressure estimation was shown.

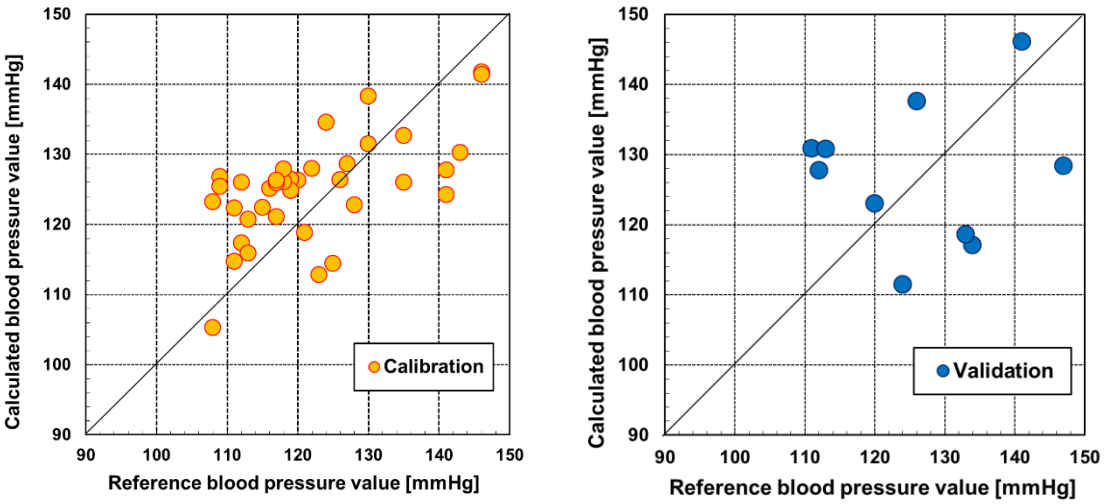

(a) SBP

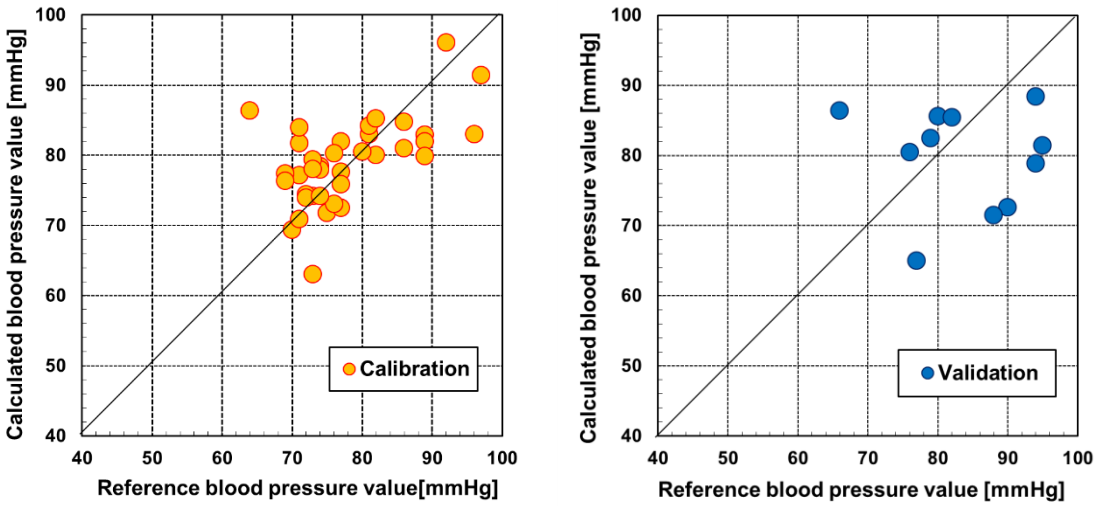

(b) DBP

Figure 5-7. Calibration curve and validation results using classified data set

Table 5-3. Calibration and validation results using classified data set

(a) SBP

Calibration			
Sample	Avg. [mmHg]	Min [mmHg]	Max [mmHg]
40	125	108	165
Result	Factor		4
	Correlation coefficient		0.43
	SEC [mmHg]		14

Validation			
Sample	Avg. [mmHg]	Min [mmHg]	Max [mmHg]
11	129	111	163
Result	SEC [mmHg]		21

(b) DBP

Calibration			
Sample	Avg. [mmHg]	Min [mmHg]	Max [mmHg]
40	80	64	102
Result	Factor		4
	Correlation coefficient		0.60
	SEC [mmHg]		8

Validation			
Sample	Avg. [mmHg]	Min [mmHg]	Max [mmHg]
11	84	66	95
Result	SEC [mmHg]		13

5.5. Conclusion

In this chapter, I classified the pulse wave signal measured by the FBG sensor into 7 patterns aiming to eliminate the shape difference of pulse wave signal and improve the estimation accuracy of blood pressure. I measured the pulse waves of multiple subjects using FBG sensor. The measured pulse waves were classified according to Sano, et al classification. Then, the calibration curves were constructed using the non-classified data and the classified data and calculated the blood pressure value. Comparing both calibration and validation results, it was shown that the pulse wave classification tended to make the correlation coefficient bigger and make SEC and SEP smaller. Which reveals that the shape difference of pulse waves and the standardization method may cause the low prediction accuracy. Therefore, it is appropriate to estimate the blood pressure value using classified pulse waves.

In this chapter, it was found that the shift of the point to be standardized to 0 is one of the factors which makes the estimation accuracy lower. Therefore, to aim more improvement of the accuracy of blood pressure value estimation, it is needed to fix the point to be standardized to 0. It is also important to confirm whether the same tendency can be observed for the estimation using pulse wave of the different pattern like as the estimation using the pulse waves classified as pattern A. In this chapter, the estimation improvement by classifying the pulse wave according to Sano et al. classification was confirmed. There are other classification methods for pulse wave. Therefore, the validations how accuracy change by other classification methods are also needed. Not only following the exist classification method, the other pulse wave classification such as

classification according to age or classification according to both age and pulse wave pattern also should be tested. As described in the previous chapter, the estimation by ANN is better than PLSR. Therefore, the estimation by ANN with the classified pulse waves is also necessary to confirm the combination of the estimation method and the data set makes the estimation accuracy better. Finding the best estimation method through these examinations, the blood pressure measurement device using FBG sensor can be realized.

5.6. References

[5-1] "Annual Report on the Aging Society: 2015 (Summary)," Cabinet Office, Government of Japan. [Online]. Available: https://www8.cao.go.jp/kourei/english/annualreport/2015/2015pdf_e.html.

[5-2] Y. Ken-Ichi, "Progress of Non-invasive, Ambulatory, and Non-conscious Biomedical Measurement," J. Jpn. Soc. Precis. Eng., vol. 62, no. 11, pp. 1525–1529, Nov. 1996, doi: 10.2493/jjspe.62.1525.

[5-3] Yahagi N., Vital care network - Life saving network, vol. 9. Nature interface, 2002.

[5-4] Tokuda Y., Dr. Tokuda's vital sign course. Japan Medical Journal, 2013.

[5-5] Y. Miyauchi, H. Ishizawa, and M. Niimura, "Measurement of Pulse Rate and Respiration Rate Using Fiber Bragg Grating Sensor," Trans. Soc. Instrum. Control Eng., vol. 49, no. 12, pp. 1101–1105, 2013, doi: 10.9746/sicetr.49.1101.

[5-6] S. Sato, M. Kawamura, Y. Miyauchi, and H. Ishizawa, "Simultaneous measurement of the pulse rate and respiratory rate by fiber Bragg grating sensors," presented at the 28th SICE Sensing Forum, Yokohama, Japan, 2011, pp. 97–100.

[5-7] Y. Miyauchi, H. Ishizawa, S. Sato, and A. Hattori, "Development of the pulse rate measuring system by FBG sensors," presented at the 10th JSMBE Symposium Nagano district, Nagano, Japan, 2012, pp. 13–14.

[5-8] Y. Katsuragawa and H. Ishizawa, "Non-invasive blood pressure measurement by pulse wave analysis using FBG sensor," presented at the 2015 IEEE International Instrument and Measurement Technology Conference (I2MTC), Pisa, Italy, 2015, pp. 511–515, doi: 10.1109/I2MTC.2015.7151320.

[5-9] S. Chino, H. Ishizawa, S. Hosoya, S. Koyama, and K. Fujimoto, "Non-invasive blood pressure measurement—The study of measuring points," presented at the SICE Annual Conference 2016, Tsukuba, Japan, 2016, pp. 1706–1709, doi: 10.3390/s17010048.

[5-10] S. Yuji et al., "Evaluation of peripheral circulation with accelerated plethysmography and its practical application. | Article Information | J-GLOBAL," J Sci. Labor, vol. 61, no. 3, pp. 129–143, 1985.

[5-11] Y. Sano and T. Yoshino, "Fast optical wavelength interrogator employing arrayed waveguide grating for distributed fiber Bragg grating sensors," J. Light. Technol., vol. 21, no. 1, pp. 132–139, Jan. 2003, doi:

10.1109/JLT.2003.808620.

[5-12] Y. Sano and T. Yoshino, “Effect of light source spectral modulation on wavelength interrogation in fiber Bragg grating sensors and its reduction,” IEEE Sens. J., vol. 3, no. 1, pp. 44–49, Feb. 2003, doi: 10.1109/JSEN.2003.809027.

[5-13] M. Todd, G. A. Johnson, and C.-C. Chang, “Passive, light intensity-independent interferometric method for fibre Bragg grating interrogation,” Electron. Lett., vol. 35, pp. 1970–1971, Nov. 1999, doi: 10.1049/el:19991328.

[5-14] S. Hinohara and S. Okada, How to see and read the vital signs. Shorinsha, 2004.

[5-15] Y. Miyauchi, S. Koyama, and H. Ishizawa, “Basic experiment of blood-pressure measurement which uses FBG sensors,” presented at the 2013 IEEE International Instrumentation and Measurement Technology Conference (I2MTC), Minneapolis, MN, USA, 2013, pp. 1767–1770, doi: 10.1109/i2mtc.2015.7151320.

Chapter 6

Conclusions

6.1. Conclusions

A daily health care or monitoring is very important both for healthy person and sick person because it shows an effect on prevention and prediction of diseases and is useful for follow-up examination. In this dissertation, the validity of the pulse wave signal measured by the FBG sensor system for the vascular age and arteriosclerosis prediction was discussed. The blood pressure value estimation which assumed the daily life was also examined. Estimation methods for blood pressure value were also investigated to attain improvement in estimation accuracy.

In Chapter 2, I focused on the shape similarity between the shape of the pulse wave signal measured by the FBG sensor and the SDPTG signal. According to the classification of Sano et al., the pulse wave signals measured by the FBG sensor were classified into seven patterns and then, it was checked how the signal shape changes according to age and the blood pressure level. The shape pattern of the pulse wave signal measured by the FBG sensor tended to indicate poor blood circulation when age increases and the blood pressure level becomes high. This tendency is the same as SDPTG signal, therefore, the verification of FBG sensor system for the vascular age and arteriosclerosis estimation was shown.

In Chapter 3, the verification whether the FBG sensor system can predict the sudden changes in blood pressure was preformed supposing the real-life situations. The pulse wave signal was measured by the FBG sensor on the wrist while simulating abrupt blood pressure change by the cold pressor test. A variation in the blood pressure values for different subjects owing to difference in rise of sympathetic nerve activity was observed. The signal processing

effectively emphasized the shape change of pulse wave signals. It was found that the shape of the pulse waves reflected from the peripheral blood vessels was notable with the blood pressure change. The sudden changes in the blood pressure were able to be traced as accurately as the gradual intra-day blood pressure fluctuations by the proposed method.

In Chapter 4 and Chapter 5, the accuracy of the blood pressure estimation was improved toward to the high versatility of FBG sensor system. In Chapter 4, two estimation methods, PLSR and ANN were compared. The individual difference of the pulse wave shape influenced the accuracy of both methods, but ANN was able to reduce the effect of the individual difference by the optimization of the combined load and the bias of the network by the repetitive leaning. ANN was more suitable for the blood pressure value estimation. In Chapter 5, the validity of the pulse wave signal classification for the blood pressure value estimation was verified. The pulse wave signals were classified into the seven patterns and the data set for the calibration curve construction was determined. The classification of the pulse wave signal was effective for the blood pressure value estimation because it reduced the effect of shape difference of the pulse wave.

6.2. Future task and prospect

The goal of this study is to contribute the improvement of quality of life and to reduce the workload of medical professionals through the development wearable multi vital sign measurement device and its diffusion. In this dissertation, the likelihood of new applications using FBG as the vascular age and arteriosclerosis estimation was validated. Moreover, for the blood pressure value estimation, it is found that our system can be used for both for gradual intra-day blood pressure fluctuations and abrupt change in blood pressure. It is also found that the ANN and the pulse wave classification were valid method tor the improvement of estimation accuracy.

However, there are various tasks to be solved. In this dissertation, I only just showed the likelihood of realization of vascular age and arteriosclerosis estimation using FBG sensor. Therefore, the comparison of the vascular age and the degree of arteriosclerosis estimated by the system and the reference value obtained by a conventional device is necessary. Moreover, the experiment with healthy subjects and subjects with circulatory system disease is also needed to acquire the data over wide ranges of vascular ages and degree of arteriosclerosis. On the other hand, for more improvement of the accuracy of blood pressure value estimation and its usability, it is needed to change the signal process and the classification method. Finding the best estimation method through these examinations, the blood pressure measurement device using FBG sensor can be realized. Furthermore, in order to solve the problem that the change in the shape of the pulse wave signal became gradual by averaging, which causes of the low accuracy, I have to use the device which takes shorter time to measure the

reference values.

To realize the proposed system as a medical instrument, it must be proved that the relationship between pulse wave signal obtained by FBG sensor and blood pressure or arteriosclerosis since the method have not been proved theoretically. Therefore, the measurement examination with an artificial blood vessel was performed and now analysing. Moreover, the placement of the FBG on the skin surface may affect the signal; hence, the placement method is also been investigating. Furthermore, the sensor install method which suitable as the wearable device also must be discussed. For this problem, the install method into the wearable textile materials that takes advantage of the sensor shape has already reported. To overcome the problem related to the interrogation unit, which limits portability and transportability, a wireless portable interrogation system employing an optical edge filter has been proposed.

As mentioned, we have already reported that the FBG sensor system can measure other vital signs such as heart rate, respiration rate, and blood glucose. Hence, combining these vital sign measurement systems with the blood pressure measurement system and the estimation method of blood vessel condition, the various vital signs can be measured by a single FBG sensor system at once. Eventually, when settle the problems above, the proposed system becomes a reliable and wearable method for an extensive and continuous monitoring of health. Moreover, installing remote communication system, a medical examination by the doctor without visiting medical establishment become possible and more robust health monitoring system is realized.

The application FBG sensor system is not limited to measure the vital

signs mentioned above. I have already performed the experiments for developing the fetal monitoring device using FBG sensor. It was confirmed that just attaching the attaching the FBG sensor on the maternal abdomen, not only the fetal heart rate but also maternal respiration rate and heart rate were can be measured at once. Moreover, applying the adaptive filter, the possibility of the extraction of fetal heart rate signal was also found. Therefore, when realize the fetal and maternal monitoring system using FBG sensor, it becomes possible to soften anxiety of the mother and in case the condition both of mother and fetus has changed suddenly, the prompt medical care can be given.

From the usefulness of the FBG sensor system described above, the proposed FBG sensor system can be used for the health monitoring from before birth to end of life; hence, our system can greatly contribute to the society, especially the medical industry.

Publications

This dissertation is based on the following published papers.

Journal of articles

- Kyoko Katayama, Shun Chino, Shintaro Kurasawa, Shouhei Koyama, Hiroaki Ishizawa, and Keisaku Fujimoto, “Classification of Pulse Wave Signal Measured by FBG Sensor for Vascular Age and Arteriosclerosis Estimation”, IEEE Sensors Journal, vol. 20, no.5, pp. 2485–2491, Nov. 2019, doi: 10.1109/JSEN.2019.2952833

- Kyoko Katayama, Shun Chino, Shohei Koyama, Hiroaki Ishizawa and Keisaku Fujimoto, “Verification of Blood Pressure Monitoring System Using Optical Fiber Sensor – Tracing Sudden Blood Pressure Changes –”, Journal of Fiber Science and Technology, vol. 76, no.2, pp. 79–87, Feb. 2020, doi: 10.2115/fiberst.2020-0008

Conference proceeding (peer review)

- Kyoko Katayama, Shouhei Koyama, Hiroaki Ishizawa, and Keisaku Fujimoto, “Improvement of Blood Pressure Prediction Using Artificial Neural Network”, 2018 IEEE International Symposium on Medical Measurements and Applications (MeMeA), Rome, Italy, pp. 223-227, June 11-13, 2018

Acknowledgements

I would like to express my heartfelt appreciation to Professor Hiroaki Ishizawa for invaluable advice, support, encouragement and giving me this research opportunity. His encouragement through my master and doctoral course made me accomplish my research and this dissertation.

Also, thanks to Assistant Professor Shouhei Koyama, Professor Keisaku Fujimoto and Professor Makoto Kanai and (Shinshu University) for giving me perceptive comments and suggestions for my research.

I also cannot help but thank the late Professor Satoshi Hosoya for warm encouragement and support.

Special thanks to my reviewers, Professor Masayuki Takatera, Professor Shigeru Inui, Professor Hiroaki Yoshida (Shinshu University), Professor Makoto Ohta (Tohoku University), and Professor Ludovic Koehl (ENSAIT) for their insightful comments and advices.

This work was supported by JSPS KAKENHI, grant number JP16H01805 and the Wearable Vital Signs Measurement System Development Project at Shinshu University. This research is (partially) supported by the Creation of a Development Platform for Implantable/Wearable Medical Devices by a Novel Physiological Data Integration System of the Program on Open Innovation Platform with Enterprises, Research Institute and Academia (OPERA) from the Japan Science and Technology Agency (JST), grant number JPMJOP1722. This work also supported by a Grant-in-Aid for the Shinshu University Advanced Leading Graduate Program by the Ministry of Education, Culture, Sports Science and Technology (MEXT), Japan.

I express much gratitude to the senior and junior members of Ishizawa-Koyama Laboratory for their supports in experiments and warm friendship, and to members of Leading Program for warm friendship. I had many meaningful and enjoyable years.

Finally, I would like to thank my beloved parent, mother Sumiyo and father Hirotaka for their understanding, patience, and sea of love over the years.